Nanosecond Pulsed Electric Fields (nsPEFs) Trigger Cell Differentiation and Transcriptional Responses in Green Microalgae

Zur Erlangung des akademischen Grades eines

DOKTORS DER NATURWISSENSCHAFTEN

(Dr. rer. nat.)

der KIT-Fakultät für Chemie und Biowissenschaften

des Karlsruher Instituts für Technologie (KIT) - Universitätsbereich

genehmigte

DISSERTATION

von

Fan Bai

aus

Jilin, China

KIT-Dekan: Prof. Dr. Willem Klopper

Referent: Prof. Dr. Peter Nick

Korreferent: Prof. Dr. Martin Bastmeyer

Tag der mündlichen Prüfung: 26th, Juli, 2017

Die vorliegende Dissertation wurde am Botanischen Institut des Karlsruher Instituts für Technologie (KIT), Botanisches Institut, für Molekulare Zellbiologe, im Zeitraum von Oktober 2013 bis Juli 2017 angefertigt.

Hiermit erkläre ich, dass ich die vorliegende Dissertation, abgesehen von der Benutzung der angegebenen Hilfsmittel, selbständig verfasst habe.

Alle Stellen, die gemäß Wortlaut oder Inhalt aus anderen Arbeiten entnommen sind, wurden durch Angabe der Quelle als Entlehnungen kenntlich gemacht.

Diese Dissertation liegt in gleicher oder ähnlicher Form keiner anderen Prüfungsbehörde vor.

Karlsruhe, 2017

Fan Bai

Acknowledgments

I would like to take this opportunity to express my gratitude to all those who helped me during my entire study.

First and foremost, I would like to express my heartfelt gratitude to my supervisor Professor Peter Nick for his helpful guidance, valuable suggestions and constant encouragement in my study. I have benefited tremendously from his critical thinking and insightful viewpoint. He provided me with beneficial help and offered me precious comments during my writing, without which my manuscript would not be published now.

I am grateful that Prof. Dr. Martin Bastmeyer agreed to be my co-examiner immediately and I really appreciate his time, devotion and expertise.

I also would like to express my sincere gratitude to Dr. Wolfgang Frey for the wonderful time that I spend in his lab at Institute for Pulsed Power and Microwave Technology (IHM), Karlsruhe Institute of Technology (KIT). My thanks also go to Dr. Christian Gusbeth, who performed and maintained a stable condition of nanosecond pulsed electric fields (nsPEFs) for our project, and he also greatly broadened my horizon and enriched my knowledge in my study. I also thank Dr. Aude, Ralf, Rüdiger for their help when I was working in IHM.

Also, I would like to thank all the doctoral students as well as all the members who work in Botanical Institute for such a pleasant, friendly and helpful working atmosphere. I thank especially Qiong Liu for her suggestion and advice during my experiment. My thanks extend to Xiaolu, Lixin, Peijie, Ye and Xiang, from them I learned many things as well as getting help and support all the way since 2013. I would thank Si, Hao, Ruipu, Pingyin, Gangliang, Peng, Junning for their help and accompany in my study and my life.

Finally, I would like to thank my parents and friends, whose encouragement and support have made my accomplishments possible.

At last, thanks to the financial supported by the China Scholarship Council (CSC) for my Ph. D study and life in Germany.

Fan Bai

Karlsruhe, 2017

Contents

Contents

Contents

VIII

ABBREVIATIONS

2, 4-D: 2, 4-dichlorophenoxyacetic acid

AMPK: AMP-activated protein kinases

Asc: ascorbic acid

BKT: β-carotene ketolase

C. reinhardtii: microalgae *Chlamydomonas reinhardtii*

crtR-b: β-carotene hydroxylase

DMAPP: dimethylallyl pyrophosphate

DMSO: dimethyl sulfoxide

DPI: diphenyl iodonium

ER: endoplasmic reticulum

FW: fresh weight

H. pluvialis: microalgae *Haematococcus pluvialis*

IAA: indolyl-3-acetic acid

IPP: isopentenyl pyrophosphate

JNK: c-Jun N-terminal kinase

KCH: kinesin with calponin homology

MAPKs: mitogen-activated protein kinases

MDA: malone dialdehyde

NAA: 1-naphthalene acetic acid

NaCl: sodium chloride

nsPEFs: nanosecond pulsed electric fields

ABBREVIATIONS

OD: optical density

PDS: phytoene desaturase

PEFs: pulsed electric fields

PI: propidium iodide

PSY: phytoene synthase

RboH: respiratory burst oxidase homolog

RGB: red, green and blue color model

ROS: reactive oxygen species

SC: secondary carotenoid

SDS: sodium dodecyl sulfate

TAP: tris-acetate-phosphate

TBA: 2-thiobarbituric acid

X

Zusammenfassung

Elektroimpulsbehandlung im ns-Bereich (ns-EIB) hat ein großes Potential für biotechnologische und medizinische Anwendungen. Allerdings sind die zugrundeliegenden biologischen Mechanismen, die die zellulären Reaktionen verursachen, ungenügend verstanden.

Die einzellige Grünalge *Chlamydomonas reinhardtii* wurde als experimentelles Modell verwendet, um die unmittelbaren Wirkungen der Elektroporation auf die zellulären und der entfalteten Stressantworten zu untersuchen, die durch ns-EIB hervorgerufen wurden. Die ns-EIB induzierte eine schnelle, aber transiente Membran-Permeabilisierung, Zellschwellung und einen massiven Ausstoß von reaktiven Sauerstoffradikalen (oxidative burst). Obwohl diese kurzfristigen Stressantworten innerhalb von 2 Stunden nach der Impulsbehandlung verschwinden, erschien einige Tage später eine zweite Welle von freigesetzten reaktiven Sauerstoffradikalen. Dies ging mit einem arretierten Zellzyklus einher. Gleichzeitig wurde die Zellexpansion stimuliert und die Zellen differenzierten sich zu dem geißellosen Palmella-Stadium. Diese zweite Welle von Sauerstoffradikalen konnte durch Hemmung der membranständigen NADPH-Oxidase RboH über den spezifischen Inhibitor Diphenyliodonium (DPI) gehemmt werden, nicht aber durch das unspezifische Antioxidans Ascorbinsäure (Asc) unterdrückt werden. Die Zugabe des natürlichen Auxins Indolessigsäure (IAA) vor der ns-EIB konnte die erhöhte Bildung des Palmella-Stadiums nicht eindämmen, obwohl IAA die spontane Bildung von Palmellen signifikant reduzierte.

In einer weiteren Studie wurde die EIB verwendet, um Biosynthese des pharmazeutisch interessanten Carotinoids Astaxanthin in der Mikroalge *Haematococcus pluvialis* zu modulieren. Hier wurde beobachtet, dass ns-EIB eine langandauernde Zellexpansion, aber auch und eine erhöhte Mortalität induziert. Außerdem wurde die Astaxanthin-Akkumulation stimuliert, dies aber

nur transient. Im nächsten Schritt wurde die Genexpression von Schlüsselenzymen der Astaxanthin-Biosynthese in Antwort auf entweder ns-EIB oder Salzstress gemessen. Zwar führten beide Behandlungen zu einer verstärkten Akkumulation von Transkripten für psy, crtR-b und bkt1, diese blieb aber im Falle der ns-EIB nur transient.

Abstract

Nanosecond pulsed electric fields (nsPEFs) have great potential for biotechnological and medical applications. However, the biological mechanisms causing the cellular responses are poorly understood.

Unicellular green microalgae *Chlamydomonas reinhardtii* was used as experimental model to investigate the immediate consequences of electroporation from the cellular and developmental responses evoked by nsPEFs. We found that nsPEFs could induce a short-term membrane permeabilization, cell swelling and oxidative burst. Although these short-term responses vanish within 2 hours after the pulse, a second wave of oxidative burst appeared several days later. At the meantime, the cell cycle halted, cell expansion stimulated and an immobile palmella stage of *C. reinhardtii* formed. This persistent oxidative burst can be suppressed by specific inhibitor diphenyl iodonium (DPI), but not by the unspecific antioxidant ascorbic acid (Asc). Natural auxin IAA was added prior to the nsPEFs treatment, but unable to mitigate the elevated formation of palmella stages induced by nsPEFs.

Then, nsPEFs was used to apply on microalgae *Haematococcus pluvialis* to investigate the cell responses and the feasibility of triggering astaxanthin biosynthesis. We observed that nsPEFs could induce a long-term cell enlargement and mortality on *H. pluvialis*, but a short-term stimulation of astaxanthin accumulation. And the gene expression of key enzymes of astaxanthin biosynthesis was measured in response to either nsPEFs or salt stress. Although both treatments led to an increase of transcription for *psy, crtR-b and bkt 1*, this remained transient in the case of the nsPEFs.

Abstract

XIV

1. Introduction

1.1. Nanosecond pulsed electric fields (nsPEFs)

1.1.1. Electroporation

For over 20 years, scientists are pursuing methods to develop the drug delivery without damaging tissues. In traditional methods of cell uptake, there are some limitations on the drug delivery, which including the efficiency of delivery, the extent of penetration into the interior organs and the increased effects on the over dosage of biological and chemical particles (Lakshmanan *et al.*, 2014). And now electroporation has developed and received great numbers of attentions as a widely used technique to transport biomolecules or other large molecules across the plasma membrane.

The theory behind electroporation is, when cell suspensions or tissues is applied with a pulse of intense external electric field (Schematic of electroporation in mammal cells, see **Fig. 1.1** (Lakshmanan *et al.*, 2014)), the plasma membrane is charging and the transmembrane potential is changed (Neumann&Rosenheck, 1972; Flickinger *et al.*, 2010). At the meanwhile, the phospholipid molecules in the lipid bilayer are massively rearrangement and generate hydrophilic pores on the plasma membrane (Chen *et al.*, 2006). And this phenomenon of transient increasing in the cell membrane permeability is defined as electroporation.
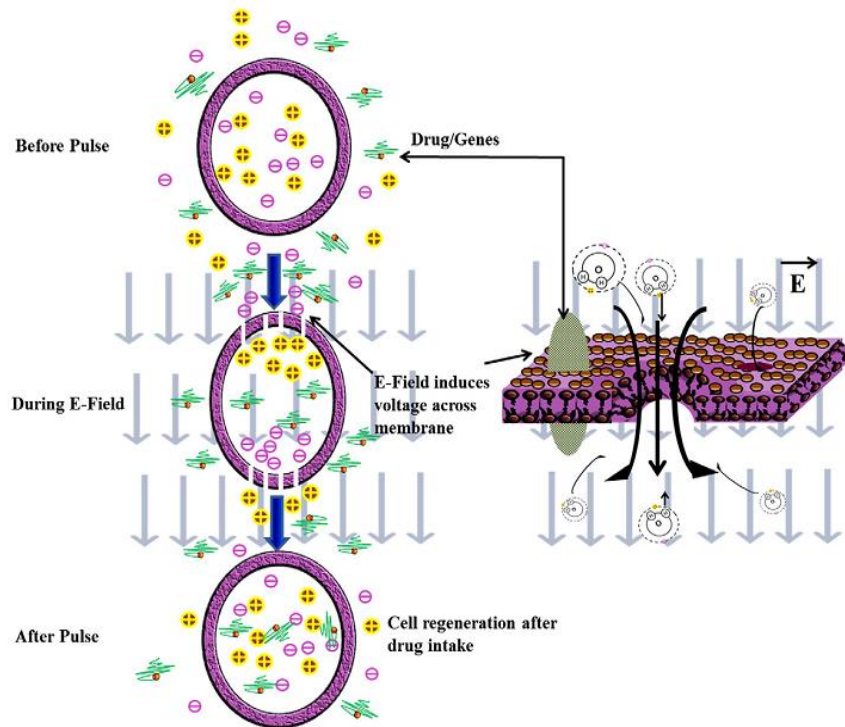
Figure 1.1: Schematic of electroporation phenomenon and the process of drug/gene deliver before, during and after pulse in mammal cells.

1.1.2. Development of pulsed electric fields (PEFs) technology

Pulsed electric fields (PEFs) is developed to generate electroporation and utilized for a wide range of applications on life sciences.

In traditional PEFs, cells or tissues are exposed under low electric field strength (a few hundred $V \cdot cm^{-1}$ to several $kV \cdot cm^{-1}$) and with pulses duration of microsecond to millisecond range. Since the induced pores which increase the permeability of the plasma membrane are large enough to allow passage of ions and macromolecules, traditional PEFs is extensively used to introduce DNA and pharmacological compounds into the target cells   (Mir *et al.*, 1991; Breton *et al.*, 2012), extract cellular ingredients   (Goettel *et al.*, 2013), and even prolong the shelf life of food   (Wouters&Smelt, 1997).

During recent years, traditional PEFs has been complemented by nanosecond

pulsed electric fields (nsPEFs). These pulses, characterized by high field strength (up to 300 kV·cm^{-1}) and extremely short pulse duration which in the nanosecond range, produce a wide variety range of interesting biological effects. One distinct characteristics of nsPEFs is, it will induce a transient and increase of membrane permeability and allows for a mild form of electroporation without affecting cell viability   (Schoenbach *et al.*, 2004), and the magnitude of the transport of ions and molecules through the plasma membrane is lower for nsPEFs treatment than traditional electroporation (Chen *et al.*, 2004). Another distinction is, in traditional PEFs, the electrical field is so mild and only effect on plasma membrane before the energy dissipated by the charging of the membrane (**Fig. 1.2** *left*), while for nsPEFs, the high electric field is able to penetrate into the cell interior before it is dissipated by charging of the plasma membrane (**Fig. 1.2** *right*) (Gowrishankar *et al.*, 2006; Akiyama&Heller, 2016).
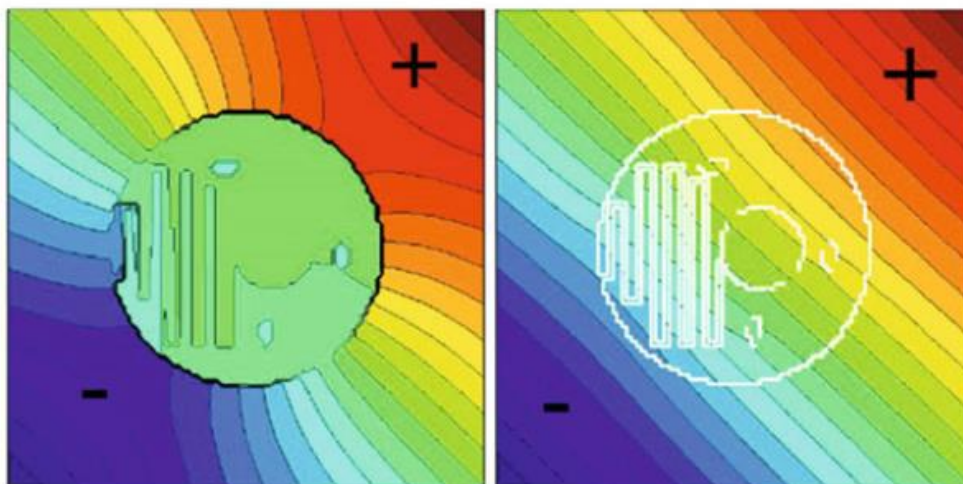
Figure 1.2: Schematic model of the effect of 7 μs long pulse duration/ 1.1 kV/cm low electric field (***left***) and 60 ns short pulse duration/60 kV/cm intense electric field (***right***) on mammal cells.

1.1.3. NsPEFs induce intracellular responses in mammal and plant cells

In recent years, more and more research have found out nsPEFs could induce intracellular responses on organelles, signaling pathways and gene expression in both mammals and plant cells.

For nsPEFs could induce reversible and irreversible membrane permeability, this is causing a transient loss of membrane cohesion, and further of phospholipid scrambling and membrane disorder (Escoffre *et al.*, 2014). Furthermore, the hydrophilic pores opened by nsPEFs causing the water uptake by cells or the osmolality disbalance of pore-impermeable solutes across the cell membrane, and this finally leading to the cell swelling (Nesin *et al.*, 2011). Besides, studies also shown that nsPEFs could causing the disassembly of actin cytoskeleton in both mammal (CHO-K1) and plant (tobacco BY2) cells (Berghöfer *et al.*, 2009; Pakhomov *et al.*, 2014), but in tobacco cells, the detachment of transvacuolar actin from the cell periphery could be inhibited by using the actin-stabilizing drug phalloidin (Berghöfer *et al.*, 2009).

NsPEFs could also trigger the response of organelles, such as inducing the membrane permeability of mitochondria and endoplasmic reticulum (ER), which leading to the increasing of the calcium influx and release (Scarlett *et al.*, 2009; Beebe *et al.*, 2012). In human cells, nsPEFs could activate the signaling pathways of mitogen-activated protein kinases (MAPKs), AMP-activated protein kinases (AMPK) and c-Jun N-terminal kinase (JNK) (Morotomi-Yano *et al.*, 2011a; Morotomi-Yano *et al.*, 2011b; Morotomi-Yano *et al.*, 2012). While in tobacco cells *Nicotiana tabacum* L. cv bright yellow 2 (BY-2), nsPEFs could activate the plant-specific KCH (kinesin with calponin homology) kinesin located on the cell membrane which response for the cell elongation and widening (Kühn *et al.*, 2013).

At last, nsPEFs even could modulate caspase activity and trigger apoptosis in mammal cells. There are two main apoptosis pathways in mammal cells which is mitochondria and endoplasmic reticulum (ER) pathway. Ling He et al.(He *et al.*, 2017) applied liver cancer cell HepG2 with 500 ns pulse duration and 10 kV·cm^{-1} field strength, then the mitochondria apoptosis pathway was activated. However, M. Yano et al.(Yano *et al.*, 2011) found out that, by treating cervical cancer cells HeLa S3 with 120 ns pulse duration (12.5 kV·cm^{-1} field strength and 100 pulse number), the gene expression of several apoptosis proteins on ER pathway were activated but not the mitochondria pathway.

There is a large amount of research focusing on the responses of mammal cells to the nsPEFs. However, the studies of nsPEFs on plant cells are few, and the biological mechanisms underlying these cellular responses are still poorly understood.

1.1.4.   Application of nsPEFs

Due to nsPEFs could induce apoptosis on cells and tissues, it is widely used in the research on the tumor and cancer therapy ((Miao *et al.*, 2015), for review, see (Chen *et al.*, 2012)). Besides, nsPEFs could induce membrane permeability, and this maybe leading to a more nutrient uptake of cells from the environment. So scientists are focusing on the study of the application of nsPEFs on the growth stimulation of plant cells, such as the increase of leaf area in *Arabidopsis thaliana* (Eing *et al.*, 2009), and improve of yield on edible mushroom (Takaki *et al.*, 2009). Besides, the application of nsPEFs is also used on the food processing (for review, see (Sack *et al.*, 2010)) and the study of valuable compound extraction from microalgae (Guionet *et al.*, 2017).

1.2. Oxidative burst

As nsPEFs could induce membrane permeability, which means the membrane integrity was disrupted. Maybe we could try to understand these intracellular responses induced by nsPEFs from the viewpoint of oxidative burst.

1.2.1. What is oxidative burst and reactive oxygen species (ROS)?

Cellular stress can assume numerous different shapes, most of the early signals are shared. One of these central stress signals is oxidative burst, whose temporal and spatial signature allows the target cell to discriminate different stress types and to respond by activation of appropriate adaptive responses   (Miller *et al.*, 2010).

Oxidative burst is generally defined as the rapid production of large quantities of reactive oxygen species (ROS) in response to the stimulation of external environment   (Mehdy, 1994). The biological function of these ROS actively produced during the oxidative burst, such as superoxide anions (O_2^-), hydrogen peroxide (H_2O_2), and hydroxyl radicals ($^.OH$)   (Wojtaszek, 1997; Bhattacharjee, 2005), is to signal the incidence of a stress condition leading to responses in cell proliferation, differentiation, but in some cases also of programmed, apoptotic, cell death   (Sauer *et al.*, 2001; Fehér *et al.*, 2008).

In plant cells, ROS can be generated via a number of routes, such as the Mehler reaction in the chloroplast   (Noctor&Foyer, 1998), the C_2 pathway of peroxisomes   (Bhattacharjee, 2005), or by an unbalanced electron transport system in the mitochondria   (Loschen *et al.*, 1973; Forman&Boveris, 1982). While these sources of oxidative burst seem to be rather linked with cellular damage and are difficult to be controlled, the central source of signaling ROS in plant cells seems to be the plasma membrane located NADPH oxidase

RboH (Respiratory burst oxidase Homolog), which is a central player in a broad range of plant stress responses (for review, see (Sagi, 2006; Xia *et al.*, 2015)).

1.2.2. RboH and auxin signaling

Over many years, reactive oxygen species (ROS) have been merely understood as result of deregulated redox balance and, thus, as indication for cellular damage (Jürgen, 2013). Meanwhile, it has become clear that ROS fulfill a second, positive, role as signals that orchestrate the cellular adaptation to stress. If something acts as a signal, its production and decay must be regulated. In fact, a specific group of NADP(H) oxidases located in the plasma membrane have emerged as central tool for "deliberate" ROS release in plants (for review, see (Marino *et al.*, 2012)). This group of enzymes, called RboH (for Respiratory burst oxidase Homolog) generates superoxide by partial reduction of oxygen, and is activated by different stress conditions, including ionic and osmotic stress as well as biotic factors. One of the central targets for superoxide seems to be plant actin (Chang *et al.*, 2015), which on the other hand is a central factor underlying membrane integrity, and this disruption of membrane integrity would increase the penetration of superoxide into the cytoplasm, such that actin which is linked with the membrane could respond to nsPEFs (Hohenberger *et al.*, 2011). This implied that nsPEFs should act on the actin cytoskeleton. In fact, nsPEFs induced the disintegration of the actin cytoskeleton in the cortex of tobacco cells, which was followed by a contraction of actin filaments towards the nucleus and a disintegration of the nuclear envelope (Berghöfer *et al.*, 2009). Also in mammalian cells, the membrane permeabilization caused by nsPEFs not only generated osmotic imbalance and cellular swelling, but also a rapid disintegration of the actin cytoskeleton (Pakhomov *et al.*, 2014). Whether these actin responses are accompanied by oxidative burst has not been, to the best of our knowledge, addressed so far.

However, pulsed electric fields in the millisecond range have been reported to cause an oxidative burst lasting till about 60 min after pulsing, thus persisting much longer than the actual electropermeabilization of only 5 min   (Sabri *et al.*, 1996).

Interestingly, a certain ground level of superoxide is also required for normal growth and development. For instance, the signaling of the central plant hormone auxin requires superoxide to activate small G-proteins of the Rac/Rop family that will subsequently activate the important signaling hub phospholipase D   (Wu *et al.*, 2011). This molecular link between stress and auxin signaling provides a mechanism to explain how ROS can modulate important biological functions, such as cell proliferation, differentiation and induction of programmed cell death, the plant version of apoptosis (Sauer *et al.*, 2001; Fehér *et al.*, 2008). When superoxide is not consumed for auxin signaling, this will alter the activity of phospholipase D. Since the different products generated by phospholipase D can sequester different actin-associated proteins, such as the actin-capping proteins and the actin-depolymerization factors, stress-dependent stimulation of the RboH will modulate dynamics and organization of cortical actin, which in turn is a central switch for arrest of the cell cycle and initiation of cell differentiation including programmed cell death as one of the possible outputs (Chang *et al.*, 2015). This sequence of events can be mitigated by addition of auxin, because this will recruit the otherwise excessive superoxide from RboH activation for auxin signaling, thus preserving dynamics and organization of cortical actin.

1.2.3. Quantification of oxidative burst by malone dialdehyde (MDA)

To quantify the amplitude of oxidative burst, the so called MDA assay has been used extensively. This assay makes use of the fact that ROS oxidize the fatty

acids of membrane unsaturated lipids (lipid peroxidation), yielding as products conjugated dienes, hydroperoxides, and malone dialdehyde (MDA), which can be quantified by a colorimetric assay (Varghese&Naithani, 2008). However, superoxide, generated by RboH, is also used for signaling of the plant hormone auxin and therefore links the stress response with a modulation of growth and proliferation (Wu *et al.*, 2011).

To follow time courses for the cellular responses to nsPEFs, it is necessary to quantify them. Although it is possible to visualize superoxide by fluorescent dyes such as dihydrorhodamine 123 (Henderson&Chappell, 1993), it is experimentally demanding to quantify this based on quantitative image analysis. Moreover, the fluorescent detection is hampered by the strong autofluorescence of chlorophyll present in the green microalgae such as *Chlamydomonas*. As alternative, the downstream effect of superoxide can be quantified (Triantaphylidès&Havaux, 2009). The superoxide anion generated by RboH is converted by superoxide dismutase into hydrogen peroxide, and hydrogen peroxide will further be converted into hydroxyl radicals in presence of divalent iron. Whereas hydrogen peroxide is not very reactive, hydroxyl radicals can extract hydrogen from fatty acids, triggering a radical chain reaction, which will culminate in the formation of MDA. At high temperature and low pH, MDA can react with 2-thiobarbituric acid (TBA) to produce a colored adduct which can be quantified by a colorimetric assay (for review, see (Janero, 1990)). Since the formation of MDA involves a chain reaction, this assay can detect the presence of superoxide at high sensitivity. However, one should keep in mind that MDA can be generated also by processes independent of lipid peroxidation. Therefore, it is crucial to include non-stressed control samples to determine the ground level of MDA prior to the stress treatment. If this condition is met, MDA is used as a marker for lipid peroxidation and reliable indicator of oxidative stress.

1.3. Motivation of this study

Due to nsPEFs could activate signaling pathways and induce cellular response in mammal cells, which has a variety of applications on cancer and tumor therapy. However, the cell responses of plant or microalgae cells to the nsPEFs stimulation are few. And the mechanisms behind these responses are also far from understood. As scientists are already start focusing on the application of nsPEFs on the stimulation of plant growth or extract valuable compounds from algae, but how exact plant or algae cells will response to nsPEFs? Whether ROS signaling is participated in the modulation of the cellular responses? Or could we utilize nsPEFs to modulate gene expression and trigger economic valuable compound biosynthesis from plant and microalgae are worth to study.

In our work, we use unicellular green microalgae *C. reinhardtii* as experimental model to investigate the short-term and long-term cellular responses to nsPEFs. To verify how nsPEFs manipulate gene expression and trigger valuable compound biosynthesis in microalgae, *H. pluvialis* is selected to perform the nsPEFs.

1.4. Microalgae *Chlamydomonas reinhardtii* (*C. reinhardtii*)

The unicellular alga *Chlamydomonas reinhardtii* (Chlorophyceae, Chlamydomonadaceae) is polar structure shape, with two apical flagella and basal chloroplast surrounding one or more pyrenoids, it also contain a prominent eyespot, usually red or orange, and have two or more contractile vacuoles. *C. reinhardtii* represents strongly proliferates in both liquid culture or on solid agar medium and can be controlled by various environmental signals (Erickson *et al.*, 2015)(**Fig. 1.3**). However, when living on solid medium, cells are often seen in gelatinous masses similar to those of the algae *Palmella* or *Gloeocystis* in the order Tetrasporales. Although it is unicellular, this species is

capable of distinct developmental responses. For instance, it can, in response to osmotic stress, shed the flagellae and remain ensheathed in a protective gelatinous matrix, the palmella stage; besides, during the sexual reproduction, the palmella stage could also be triggered by some environment factors, such as depletion of nitrogen, light and temperature (Sahoo&Seckbach, 2015).

As part of the ancestral line for the land plants, it has been extensively studied as model organism for photosynthesis, gene expression (Rochaix, 1995;2002), or for flagellar assembly and motility (Silflow&Lefebvre, 2001). In addition, *C. reinhardtii* has been used as cellular factory for the production of biochemicals for food, aquaculture and pharmaceutical industries, or for recombinant proteins (Spolaore *et al.*, 2006; Skjånes *et al.*, 2012).

Figure 1.3: *C. reinhardtii* cultivation in liquid medium (*left*) and agar medium (*right*).

1.5. Microalgae *Haematococcus pluvialis* (*H. pluvialis*)

Haematococcus pluvialis (Chlorophyceae, Haematococcaceae) is unicellular freshwater alga, and regarded as the best potential source of natural astaxanthin production (Boussiba *et al.*, 1999).

The growth of *H. pluvialis* can be divided into two stages, when the living environment is favorable, the cell is in green vegetative stage (**Fig. 1.4A**), and the cell morphology is pear-shaped with a diameter ranging from 8 to 50 μm.

The structure of vegetative cell contains two motile flagella, a cup-shaped chloroplast, a nucleus and an anterior eyespot (Boussiba, 2000). However, when the growing conditions become unfavorable, such as exposure under high light intensity, nutrient deficiency (nitrogen or phosphate), high salinity and high temperatures (Boussiba&Vonshak, 1991; Kobayashi *et al.*, 1997b; Wan *et al.*, 2014), the cell morphology changes distinctly, for instant, the cell shape becomes spherical and the flagella releases, the cell volume increasing and a thickened, heavy resistant cell wall is formed, besides, the cell division is also retarded (**Fig. 1.4B**) (Lemoine&Schoefs, 2010). Furthermore, the cell enters into a non-motile encystment stage and the astaxanthin starts to accumulation (**Fig. 1.4C**).
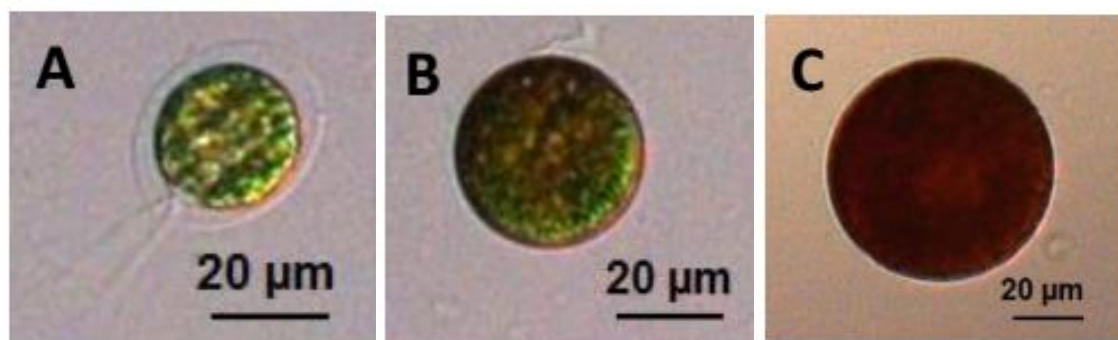
Figure 1.4: Cell morphology changes from green vegetative stage to red cyst stage during the astaxanthin accumulation in *H. pluvialis*. **A** Green vegetative cell. **B** Cell releases flagella and prepares to turn to encystment. **C** Red cysts cell with astaxanthin accumulation.

1.5.1. What is astaxanthin?

Astaxanthin (3, 3'-dihydroxy-β, β'-carotene-4, 4'-dione) is a red secondary carotenoid (SC) contains 13 conjugated double bonds (chemical formula see **Fig. 1.5** (Lemoine&Schoefs, 2010)). It contains highly antioxidant activity, and has ability to neutralize free radicals and quench ROS in response to the environment stimulation (Shimidzu *et al.*, 1996).

12
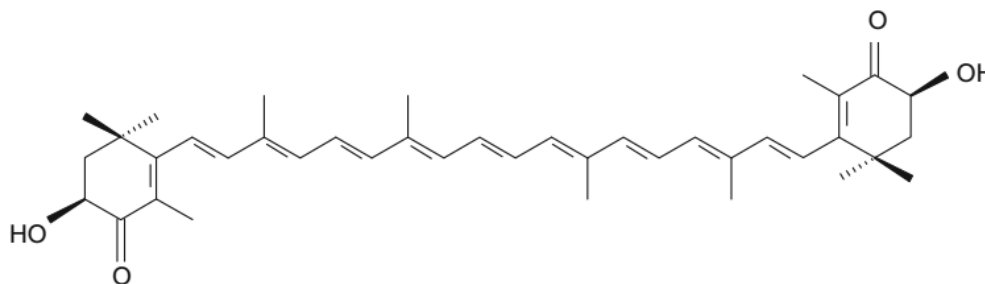
Figure 1.5: Molecular structure of nature astaxanthin.

In plant cells, primary carotenoid is essential for the basic metabolism of the organism and plays important roles in light harvesting, quenching singlet oxygen and stabilize structure during photosynthesis in the chloroplasts (Frank&Cogdell, 1996). However, secondary carotenoid is not responsible for all the metabolic functions as primary carotenoid, it accumulates in flower or fruits under specific stages of development and in response to extreme environmental conditions (Grunewald *et al.*, 2001).

Astaxanthin serves as secondary carotenoid pigment, is widely used as food colorant, feed supplement for salmon and shrimp in aquaculture industry (Christiansen *et al.,* 1995)(for review, see (Lorenz&Cysewski, 2000)). Due to the powerful antioxidant properties, astaxanthin also attracts highly interested in medical science in anti-inflammatory, cardiovascular disease therapy, anti-cancer and immune responses (Tanaka *et al.*, 1994; Bennedsen *et al.*, 2000; Guerin *et al.*, 2003; Fassett&Coombes, 2012).

Actually, only a few bacteria (*Agrobacterium aurantiacum* (Yokoyama&Miki, 1995), *Paracoccus carotinifaciens sp. nov.* (Tsubokura *et al.*, 1999)), yeast (*Phaffia rhodozyma* (Andrewes *et al.*, 1976)), plants (Ralley *et al.*, 2004; Huang *et al.*, 2013) and green algae (*Chlamydomonas nivalis*, *Chlorococcum sp.*, *Dunaliella sp.*, *Haematococcus pluvialis*, *C. zofingiensis* (Kobayashi *et al.*, 1991; Zhang *et al.*, 1997; Orosa *et al.*, 2000; Remias *et al.*, 2005; Raja *et al.*, 2007)) have the ability to synthesis astaxanthin. But among them, unicellular

algae *H. pluvialis* is found to be the best producer of astaxanthin, for it contains a highly ability of accumulation which can reach up to about 4 % of its dry cell weight (Boussiba *et al.*, 1999).

1.5.2. Astaxanthin biosynthesis pathway in *H. pluvialis*

In *H. pluvialis,* astaxanthin is synthesized in the chloroplasts and stored in the cytoplasmic lipid vesicles (Boussiba, 2000; Grunewald *et al.*, 2001). The biosynthesis pathways are shown in **Fig. 1.6** (chloroplast) and **Fig. 1.7** (cytoplasm)(Lemoine&Schoefs, 2010).

In the chloroplasts, the formation of β-carotene is generally divided into four steps (**Fig. 1.6**): (a) the universal active isoprenoid precursor isopentenyl pyrophosphate (IPP) and dimethylallyl pyrophosphate (DMAPP) are formed as the basic building blocks for astaxanthin; (b) three IPP molecules with DMAPP are condensation and then catalyzed by phytoene synthase (PSY) to form the colorless carotenoid phytoene; (c) after successive desaturation reactions of phytoene which catalyzed by phytoene desaturase (PDS), Lycopene is formed; (d) after cyclization reactions, β-carotene is generated and then transported out of chloroplast into cytoplasm to involve in the formation of astaxanthin, for review, see (Lemoine&Schoefs, 2010).

The conversion of β-carotene into astaxanthin in *H. pluvialis* is carried out in cytoplasm by two putative pathways (**Fig. 1.7**): one is started with catalysis of β-carotene by β-carotene ketolase (BKT) to form canthaxanthin and then hydroxylation by β-carotene hydroxylase (crtR-b); another is to via zeaxanthin by hydroxylation (crtR-b) and then subsequent oxidation by BKT (for review, see (Lemoine&Schoefs, 2010)). Until this step, the synthesized astaxanthin are free astaxanthin molecules, they must undergoes esterification reaction to form astaxanthin ester and finally storage in the lipid vesicles (Grunewald *et al.*, 2001; Holtin *et al.*, 2009; Chen *et al.*, 2015).
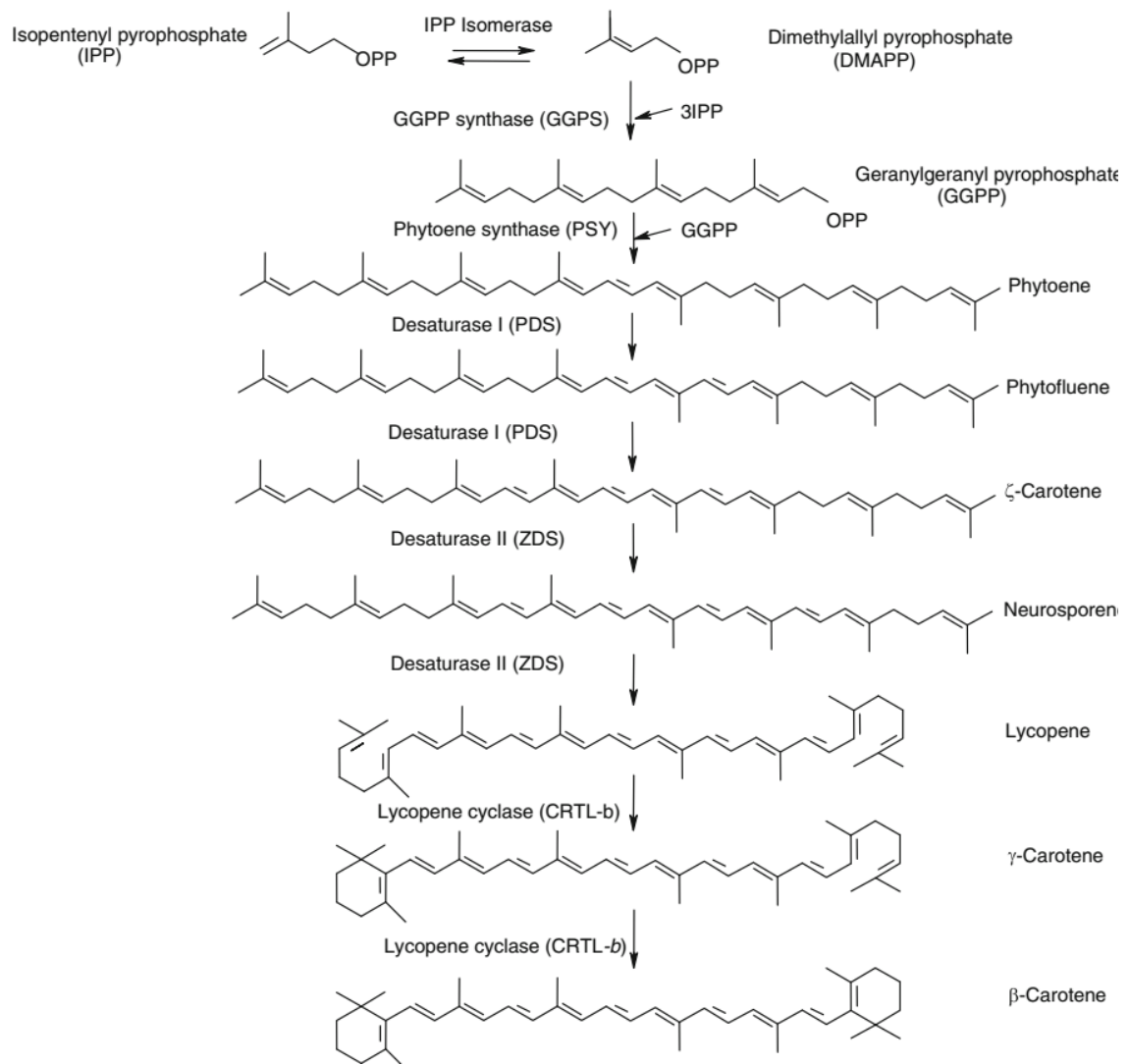
Figure 1.6: First part of astaxanthin biosynthesis pathway carried out in the chloroplast of *H. pluvialis,* the formation of β-carotene.
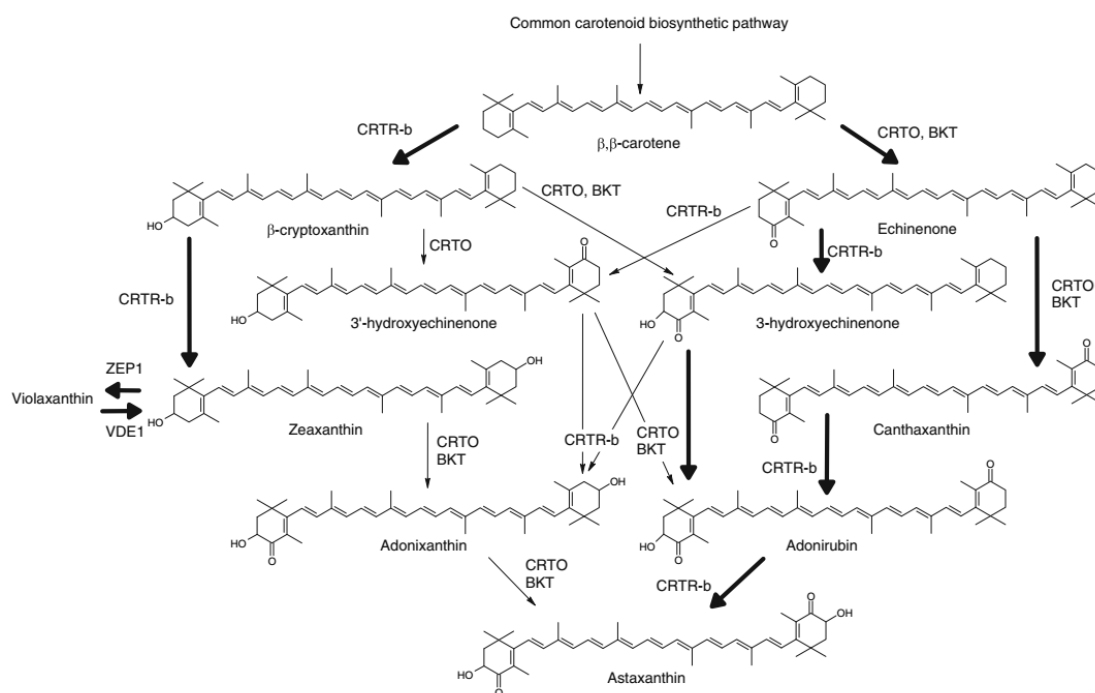
Figure 1.7: Second part of astaxanthin biosynthesis pathway carried out in the cytoplasm of *H. pluvialis*, the conversion of β-carotene to astaxanthin.

1.5.3. Enzymes involved in astaxanthin biosynthesis

In order to understand the mechanism of astaxanthin biosynthesis and improve the astaxanthin production yields, more and more researchers are focusing on the modulation of astaxanthin biosynthesis enzymes and genes, and their application on metabolic engineering.

By comparing the chemical formula of β-carotene and astaxanthin (**Fig. 1.7**), we could found out, the formation of astaxanthin need the introduction of hydroxyl groups to produce 3, 3'-hydroxylase (Linden, 1999) end and keto groups to product 4,4'-ketolase end (Kajiwara *et al.*, 1995). β-carotene hydroxylase (crtR-b) and β-carotene ketolase (BKT) are two important enzymes involved in the conversion of β-carotene into astaxanthin, and the genes had already been cloned and studied (Kajiwara *et al.*, 1995; Linden,

1999). Enzyme BKT contains three different *bkt* genes, *bkt 1*, *bkt 2* and *bkt 3*. Gene *bkt 2* and *bkt 3* shares 95 % identical nucleotide sequence and are isolated from *H. pluvialis* Flotow NIES-144 (Kajiwara *et al.*, 1995; Huang *et al.*, 2006), and *bkt 1* is isolated from *H. pluvialis* strain 34/7 (Lotan&Hirschberg, 1995).

Enzyme crtR-b and BKT could all be up-regulated at the mRNA level during the astaxanthin biosynthesis under stress conditions (Steinbrenner&Linden, 2001; Lu *et al.*, 2010). Steinbrenner and Linden(Steinbrenner&Linden, 2001) also found out that, the up-regulated of crtR-b and phytoene synthase (PSY) are independent of *de novo* protein biosynthesis, which after the addition of the protein biosynthesis inhibitor cycloheximide at 2 h prior to the stress induction, the expression of gene *psy* and *crtR-b* were still high, but the cyst cells formation and the astaxanthin biosynthesis were inhibited.

1.6. Content of this study

1.6.1. How *C. reinhardtii* responses to the stimulation by nsPEFs

To address, whether nsPEFs can modulate the balance between proliferation and stress responses, it is necessary to use experimental models with vigorous proliferation that are amenable to electropulse treatment, which is technically easier to achieve for unicellular systems rather than for multicellular organisms. We therefore used unicellular green microalgae *C. reinhardtii* to investigate the role of oxidative burst for the cellular and developmental responses induced by nsPEFs. To dissect the acute consequences of electroporation from the developmental cellular responses triggered by the signaling elicited by nsPEFs, both short-term (over the first 2 hours after the nsPEFs treatment), and long-term (over several days after the nsPEFs treatment) responses were investigated. The responses were monitored by

quantifying cell size, mortality, optical density (OD), membrane permeability, and lipid peroxidation as readout for the amplitude of oxidative burst. To modulate the oxidative burst generated by nsPEFs, we used either diphenyl iodonium (DPI), a specific inhibitor of membrane-located NADPH oxidases (Cross&Jones, 1986), or the non-specific antioxidant ascorbic acid (Asc). Using this approach, we can show that nsPEFs induce a short-term permeabilization of the membrane, linked with a transient swelling and a transient oxidative burst. Although these responses vanish within the first 2 hours after the pulse, they induce a developmental response which becomes manifest only several days later. This developmental response consists of halted cell cycle, stimulation of cell expansion, a strong oxidative burst, which is driven by the NADPH oxidase RboH, and the stimulation of palmella stages. Induction of a persistent oxidative burst by salinity stress can phenocopy the developmental response to nsPEFs. The transition point from cycling into cell expansion can be modulated by manipulation of auxin signaling, and auxin can also suppress the spontaneous transition into the palmella stage. However, auxin cannot suppress the induction of palmella formation by nsPEFs. We arrive at a working model, where the temporary permeabilization of the plasma membrane by nsPEFs treatment activates the membrane located NADPH oxidase RboH, generating apoplastic superoxide, which then triggers a developmental response whose biological context is adaptation to (osmotic) stress.

1.6.2. How nsPEFs manipulate the astaxanthin biosynthesis in *H. pluvialis*

As nsPEFs could trigger a serious of short-term and long-term cellular responses in *C. reinhardtii*, most importantly, nsPEFs could induce halted cell cycle and a long-lasting oxidative burst several days later. Due to unicellular green microalgae *H. pluvialis* could accumulate a highly antioxidant compound

named astaxanthin under several abiotic stresses. During the biosynthesis of astaxanthin, the cell morphology was changed and accompanied with ceased of cell division. Now we come to a hypothesis, which to use nsPEFs as abiotic stress to trigger the astaxathin biosynthesis in *H. pluvialis* before the cells initiate the biosynthesis naturally. To investigate a long-term cellular response and astaxanthin biosynthesis to nsPEFs, 5 days old *H. pluvialis* were used as experimental model in this part, the cell mortality and astaxanthin product were determined at 18, 24, 48, 72 and 96 h after nsPEFs treatment. To deeply explore the gene expression on transcript level in response to nsPEFs during the astaxanthin biosynthesis, the relative transcript level of gene *psy*, *crtR-b* and *bkt 1* were quantified by real-time qPCR. To further compare the differences of cellular responses between nsPEFs and abiotic stress treatment. Salt stress was used as one of the abiotic stress to trigger astaxanthin accumulation. 100 mM and 200 mM NaCl as final concentration in our experiment were used on 5 days old *H. pluvialis*, and the MDA content, cell mortality, cell diameter and astaxanthin production were quantified at 8, 24, 48, 72 and 96 h after salt stress. And the relative expression of gene *psy*, *crtR-b* and *bkt 1* were also measured at corresponding time point. And we concluded that, nsPEFs could transient manipulate the transcript level of *psy*, *crtR-b* and *bkt 1*, but there is no obvious effect on astaxanthin accumulation. And among *psy*, *crtR-b* and *bkt 1*, the relative expression of gene *bkt 1* was increased under both nsPEFs and salt treatment, which may play a more activate role than *psy* and *crtR-b* during the astaxanthin biosynthesis.

2. Materials and Methods

2.1. Cell cultivation

2.1.1. *Chlamydomonas reinhardtii* (*C. reinhardtii*) cultivation

One microalgae strain used in this study was *Chlamydomonas reinhardtii* 137c, isolated in 1945 near Amherst, MA (Proschold, 2005), obtained from the *Chlamydomonas* collection (www.chlamycollection.org). Cells were grown and maintained in 30 ml of fresh, sterilized Tris-Acetate-Phosphate (TAP) medium (Gorman&Levine, 1965; Harris, 1989)(for details, see **Table 2.1**) in a 100 ml Erlenmeyer flask. A continuous white illumination was provided by a custom-made light source consisting of a LED array placed on a cooler fabricated of aluminum and a power supply (VLP-2403; Voltcraft, Germany)(for details, see **Fig. 2.1**). The fluence rate of the light was 45 $\mu mol^{.}m^{-2.}sec^{-1}$ photosynthetically radiation, and cells were maintained with continuous rotation of 150 rpm on an orbital shaker (KS260 basic; IKA Labortechnik, Staufen, Germany) under 25 °C cultivated temperature. To standardize culture growth, a standardized number of stationary cells were inoculated yielding an initial optical density (OD) of 0.05. Under these conditions, the duration of the cultivation cycle was 7 days. As backup, *C. reinhardtii* cells were streaked on the TAP medium solidified by 1.5 % (w/v) agar (gel strength: 950-1050 $g \cdot cm^{-2}$) and subcultured every 20 days.

Table 2.1 Components of TAP medium for *C. reinhardtii*

Stock Solution (SL)	Volume/L	Component	Concentration in SL
Tris base	2.42 g	$H_2NC(CH_2OH)_3$	
		Tris(hydroxymethyl)-aminomethan	
Acetic acid	1 mL	CH_3COOH	
Phosphate solution	1 mL	K_2HPO_4	28.8 g/100 mL
		KH_2PO_4	14.4 g/100 mL
Trace elements	1 mL	$Na_2EDTA \cdot 2H_2O$	5.0 g/100 mL
		$ZnSO_4 \cdot 7H_2O$	2.20 g/100 mL
		H_3BO_3	1.14 g/100 mL
		$MnCl_2 \cdot 4H_2O$	0.50 g/100 mL
		$FeSO_4 \cdot 7H_2O$	0.50 g/100 mL
		$CoCl_2 \cdot 6H_2O$	0.16 g/100 mL
		$CuSO_4 \cdot 5H_2O$	0.16 g/100 mL
		$(NH_4)_6Mo_7O_{24} \cdot 4H_2O$	0.11 g/100 mL
TAP-salts	25 mL	NH_4Cl	15.0 g/L
		$MgSO_4 \cdot 7H_2O$	4.0 g/L
		$CaCl_2 \cdot 2H_2O$	2.0 g/L
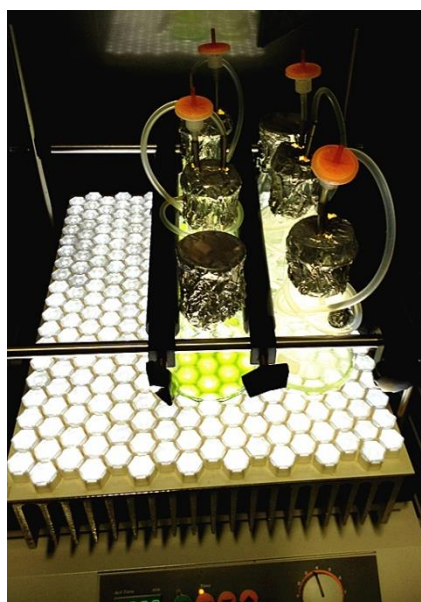
Figure 2.1: Schematic of custom-made light source for *C. reinhardtii*.

2.1.2. *Haematococcus pluvialis* (*H. pluvialis*) cultivation

Haematococcus pluvialis (*H. pluvialis*) SAG 192.80 was obtained from the Culture Collection of Algae at the Göttingen University, Germany. *H. pluvialis* were grown in 40 ml sterilized basal medium (pH 6.8) (Kakizono *et al.*, 1992)(for details, see **Table 2.2**) in a 100 ml Erlenmeyer flask under continuous white illumination light (L 36W/965; OSRAM, Germany) with a fluence rate of 25 µmol·m^{-2}·sec^{-1}. The cell suspensions were maintained in 25 °C and manually shaking once per day. The OD of initial inoculated yield was 0.1 from a standardized of stationary cells. The cultivation cycle was 7 days. *H. pluvialis* cells were streaked on the basal medium which solidified by 2 % (w/v) agar (gel strength: 950-1050 g·cm^{-2}) and subcultured every 30 days for backup.

Table 2.2 Components of basal medium for *H. pluvialis*

Component	g/L
Sodium acetate	1.20
L-asparagine	0.40
Yeast extract	2.00
$MgCl_2 \cdot 6H_2O$	0.20
$FeSO_4 \cdot 7H_2O$	0.01
$CaCl_2 \cdot 2H_2O$	0.02

2.2. Nanosecond pulsed electric fields (nsPEFs)

2.2.1. Basic experiment set up of nsPEFs

The details on the pulsed generator system was reported in previous work (Eing *et al.*, 2009; Goettel *et al.*, 2013) and for details see **Fig. 2.2**.
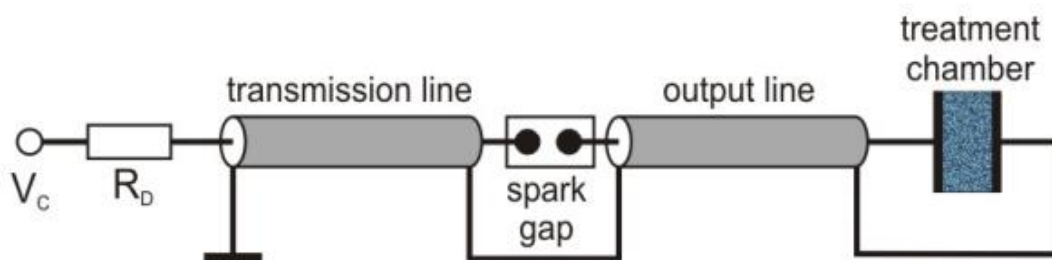
Figure 2.2: Schematic of the transmission line generator for nsPEFs.

Thirty ml of algal suspensions were treated with nsPEFs in a treatment chamber. The custom-made treatment chamber consisted of two stainless steel electrodes with a diameter of 60 mm, oriented in parallel and separated by a gap integrated into a transparent polycarbonate housing (**Fig. 2.3**). The distance between the electrodes is 2 mm and the treatment volume is 0.5 ml.

The detailed experiment set up for nsPEFs treatment was shown in **Fig. 2.4**. The cell suspensions passed the treatment chamber from the bottom via a sterilized silica rubber tubing driven by a peristaltic pump (Ismatec Ism 834C, Switzerland) at a constant flow rate. After passing the outlet at the top of the chamber, the suspension was collected in an empty, sterilized 100 ml Erlenmeyer flask sealed by a silicone plug. In this work, the transmission line pulse generator delivered rectangular pluses with a voltage amplitude of 8 kV, corresponding to the electric field strength of 40 kV·cm^{-1} (**Fig. 2.5**).

Figure 2.3: Details of the treatment chamber of nsPEFs.
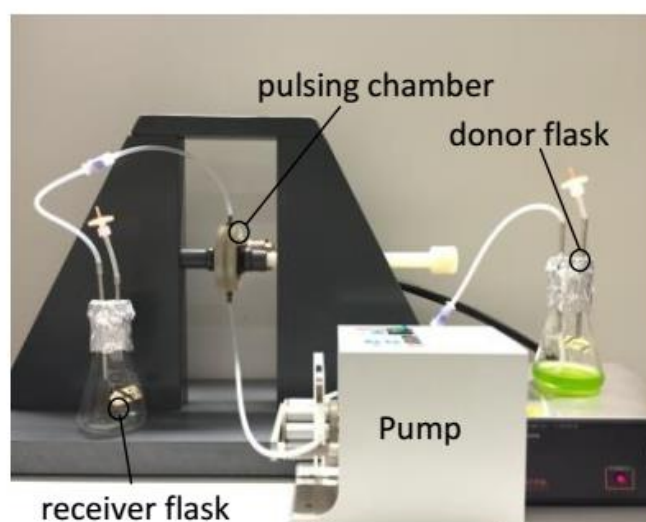
Figure 2.4: Experimental set up of pulse treatment for microalgae. The algal suspensions in the donor flask flowed into the pulsing chamber driven by a pump, after pulse treatment, cells flowed out of chamber into a sterilized receiver flask and waiting for measurement.
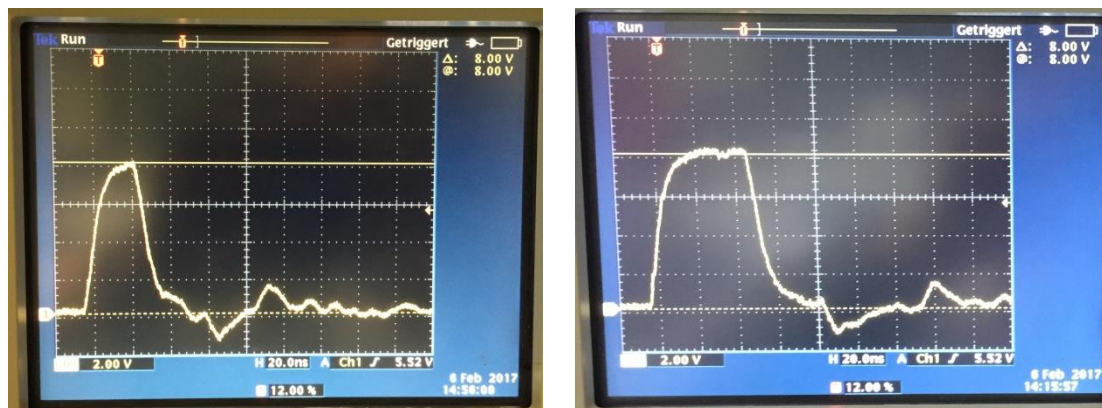
Figure 2.5: Output voltage waveforms of the transmission line generator for 25 ns (*left*) and 50 ns (*right*).

2.2.2. Experiment set up and nsPEFs parameters for *C. reinhardtii*

To investigate, whether nsPEFs can modulate the balance between proliferation and stress responses, we use unicellular alga *C. reinhardtii* as our experimental model. In this work, we investigated both short-term and long-term responses of *C. reinhardtii* to nsPEFs. To follow the short-term responses, the suspension was pulsed at day 4 after subcultivation (**Fig. 2.6,** grey arrow), for which the cell density was high enough to provide more cellular aspects of measurements. And the cell membrane permeability, cell volume and membrane lipid peroxidation were measured after nsPEFs treatment immediately. To follow long-term responses, the suspension was pulsed at 30 hours after subcultivation (when the cell was under exponential phase), in order to observe modulations happening several days later before the cells run into the stationary phase of cycle (**Fig. 2.6**, white arrow). As negative control, the suspension was cultivated and treated the same way, just omitting the application of nsPEFs. After the pulse treatment, all samples were transferred back to the incubator. And the cell optical density, cell diameter and lipid peroxidation were quantified every day.
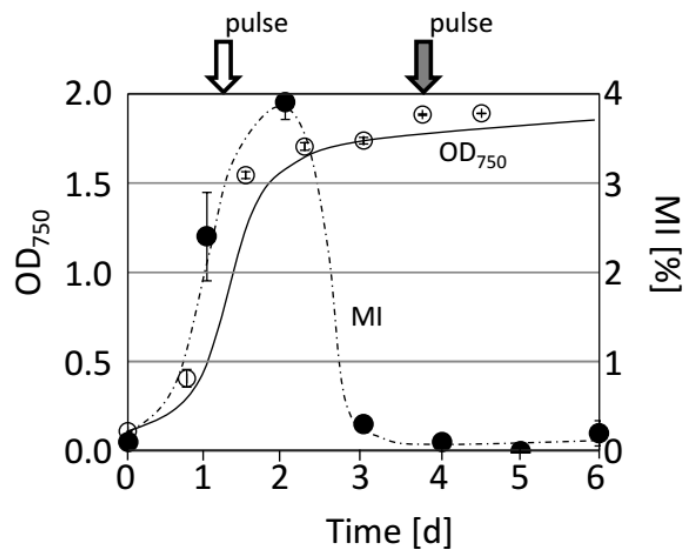
Figure 2.6: Time of the pulse treatment (arrow) in relation to the physiological parameters of the culture. The time courses of OD_{750} as measure for cell density (open circles, solid line) and mitotic index (filled circles, dashed line) are shown. Data represent mean values, error bars s_e of three independent experimental replications.

For the nsPEFs parameters used in the study of *C. reinhardtii*. The frequency of the pulses was 4 Hz and the pulse number per cell is 19. Pulses were generated in durations of 25 ns and 50 ns, which corresponding to the specific input energies of 1 $J^.g^{-1}$ and 2 $J^.g^{-1}$, respectively (**Table 2.3**).

Table 2.3 Basic parameters of nsPEFs for *C. reinhardtii*

	Field strength	Pulsed duration	TAP medium conductivity	Flow rate	Frequency	Pulse number	Input energy
1	40 $kV^.cm^{-1}$	25 ns	1.4 $mS^.cm^{-1}$	6.38 $ml^.min^{-1}$	4 Hz	19	1 $J^.g^{-1}$
2	40 $kV^.cm^{-1}$	50 ns	1.4 $mS^.cm^{-1}$	6.38 $ml^.min^{-1}$	4 Hz	19	2 $J^.g^{-1}$

2.2.3. Experiment set up and nsPEFs parameters for *H. pluvialis*

To verify, whether nsPEFs could serve as a stress factor to trigger and modulate the biosynthesis of astaxanthin in *H. pluvialis.* 5 days old cell suspensions were used as experiment model to perform the nsPEFs, which the cell was at the beginning of the stationary phase, and the astaxanthin were started to accumulate (**Fig. 2.7**, black arrow).
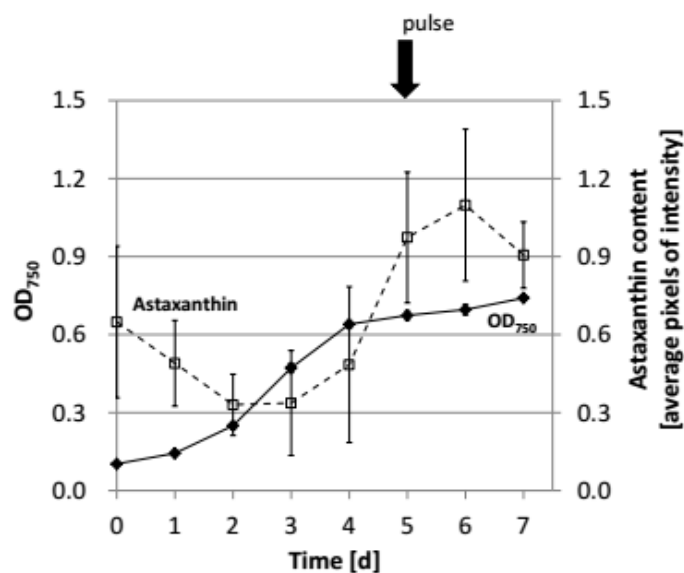
Figure 2.7: Time of the pulse treatment (arrow) in relation to the physiological parameters of the culture. The time courses of OD_{750} as measure for cell density (filled diamonds, solid line) and astaxanthin content (open squares, dashed line) are shown. Data represent mean values, error bars s_e of three independent experimental replications.

After the pulse treatment, all samples were transferred back to the incubator, and the cell mortality, cell diameter and astaxanthin content were measured at 18, 24, 48, 72 and 96 h after nsPEFs. To study the expression of the astaxanthin biosynthesis genes in response to the stimulation by nsPEFs, the transcript level of three key genes from enzyme β-carotene ketolase (*bkt 1*), β-carotene hydroxylase (*crtR-b*) and phytoene synthase (*psy*) were quantified.

To determine, whether nsPEFs could play as a stress factor to trigger and modulate the astaxanthin biosynthesis, we used salt stress to trigger the astaxanthin biosynthesis, and comparing the difference of astaxanthin accumulation and gene expression between salt stress and nsPEFs stimulation.

The nsPEFs parameters used for *H. pluvialis* was modified from the study of *C. reinhardtii*. And the details of the nsPEFs parameters were shown in **Table 2.4**. The number of pulses for *H. pluvalis* was increased to 32, and pulse duration was 25 ns and 50 ns and the final input energy were 2 $J \cdot g^{-1}$ and 4 $J \cdot g^{-1}$, respectively.

Table 2.4 Basic parameters of nsPEFs for *H. pluvialis*

	Field strength	Pulsed duration	Basal medium conductivity	Flow rate	Frequency	Pulse number	Input energy
1	40 $kV \cdot cm^{-1}$	25 ns	1.6 $mS \cdot cm^{-1}$	3.75 $ml \cdot min^{-1}$	4 Hz	32	2 $J \cdot g^{-1}$
2	40 $kV \cdot cm^{-1}$	50 ns	1.6 $mS \cdot cm^{-1}$	3.75 $ml \cdot min^{-1}$	4 Hz	32	4 $J \cdot g^{-1}$

2.3. Optical density (OD)

One ml cell suspension was taken in a cuvette, and the optical density (OD) was determined by a UV-Vis Spectrophotometer (Uvikon XS, Goebel Instrumentelle Analytik GmbH, Germany) under the wavelength of 750 nm. Data represent mean values of three replications and standard errors of three independent experimental series.

2.4. Mortality assay

To quantify viability, the membrane-impermeable dye Evan's Blue was used (Gaff&Okong'O-Ogola, 1971; Kühn *et al.*, 2013). Two ml of cell suspension was spun down in a 2.0 ml reaction tube (Eppendorf, Hamburg) at 4,000×g for 2 min (PICO 17, Thermo Scientific, Germany), then, the supernatant was replaced by 1 ml of 2.5 % Evan's Blue (w/v, dissolved in double distilled water). After staining for 5 min, the dye was removed by centrifugation at 4,000×g for 2 min. Then, 1 ml of fresh cultivation medium (TAP medium for *C. reinhardtii*, and basal medium for *H. pluvialis*) was added and vortexed briefly to remove the unbounded dye. This was repeated until the supernatant was colorless. Finally, the cells were resuspended in 250 µl of fresh cultivation medium. Aliquots of 20 µl were quantified in a hematocytometer (Fuchs-Rosenthal) under an ApoTome microscope (AxioImager Z.1; Zeiss, Germany) using a 63× oil immersion objective for *C. reinhardtii* cells, and an Axioskop microscope (Axioskop 2 FS; Zeiss, Germany) using a 20× objective for *H. pluvialis* cells. At least 1,500 cells were quantified for each measurement. Data represent mean values and standard errors of three independent experimental series.

2.5. Quantification of membrane permeability of *C. reinhardtii*

To determine, whether the plasma membrane was transiently permeabilized due to the application of nsPEFs, Evan's Blue was used as a marker, for which *C. reinhardtii* contains chlorophyll which is red fluorescent and therefore covering the signal of other dyes such as propidium iodide (PI). Living cells exclude Evan's Blue, but transient formation of membrane pores in response to nsPEFs should allow the uptake of Evan's Blue. The protocol for staining was the same as given in Morality assay, but the dye was added at specific time intervals after pulsing. At least 1,500 cells were quantified for each

30

measurement. Data represent mean values and standard errors of three independent experimental series.

2.6. Quantification of cell volume of *C. reinhardtii*

To get statistic information about changes in cell size, an automatic particle counter system (CASY® Model TT System version 1.1, Roche Diagnostics GmbH, Germany)(**Fig. 2.8**) was employed. To exclude that particle debris would cause undesired background, each measurement was preceded by a cleaning procedure, whereby the measuring capillary was flooded by 10 ml of CASY® buffer (Roche Diagnostics) following the instructions of the producer. This step was repeated until the cell counts in each sample were below 200 per ml, before a new sample was measured. Aliquots of 50 µl of *C. reinhardtii* cell suspension were diluted in 10 ml of buffer and measured, collecting the data by means of the CASY excel 2.4 Software. Data represent mean values and standard errors from three independent experimental series. Volumes were inferred from the size distribution based on the assumption that the cells are spherical.
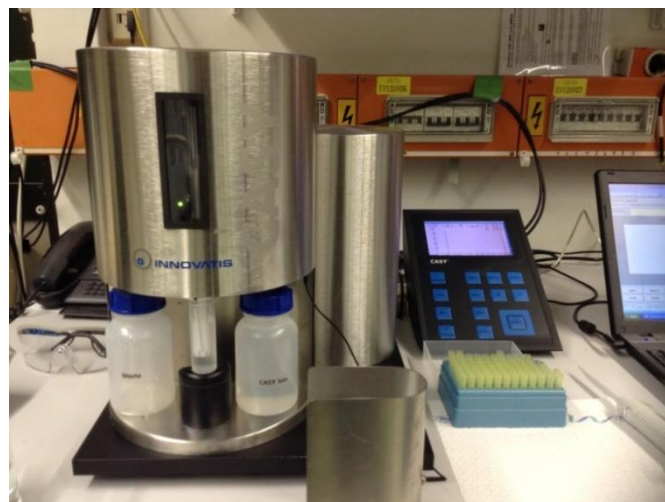
Figure 2.8: Device of cell counter system for the quantification of cell volume of *C. reinhardtii*.

2.7. Quantification of lipid peroxidation by malone dialdehyde (MDA)

To quantify lipid peroxidation as readout for oxidative burst, the reaction product MDA was measured by using the reaction between MDA and 2-thiobarbituric acid (TBA) yielding a colored adduct following a protocol published for plant cells (Hodgson&Raison, 1991) with minor modification: Two ml of cell suspension was added into an empty and pre-weighed reaction tube (2.0 ml, Eppendorf, Hamburg), the supernatant was removed after spun down for 4 min at 10,000×g. By weighing the filled tube again, fresh weight of the cells was determined. Then, the cells were shock-frozen in liquid nitrogen immediately. A sterilized steel bead was added into the sample, and then the frozen cells was homogenised twice by a Tissuelyser (Qiagen, Retsch, Germany) at 18 Hz for 30 seconds. After addition of 1 ml 0.1 M phosphate buffer (pH 7.4) and centrifugation at 8,000×g for 4 min, 200 µl of the supernatant were transferred into a mixture containing 750 µl of 20 % (v/v) acetic acid, 750 µl of 0.8 % (w/v) TBA, 200 µl of Milli-Q water, and 100 µl of 8.1% (w/v) sodium dodecyl sulfate (SDS). As blank, the 200 µl of supernatant was replaced by an equal volume of 0.1 M phosphate buffer. Subsequently, both specimen and blank were incubated at 98 °C for 1 h. After cooling down to room temperature, the absorbance at 535 nm was measured in a UV-Vis Spectrophotometer (Uvikon XS, Goebel Instrumentelle Analytik GmbH, Germany) and corrected against the absorbance at 600 nm monitoring unspecific background. The content of MDA ($\mu M^{\cdot}g$ FW^{-1}) could be calculated by

$$\text{MDA } (\mu M^{\cdot}g \text{ FW}^{-1}) = [(A_{535}-A_{600})/155000] \times 10^{6}/\text{Fresh weight,}$$

Data represent mean values and standard errors from three independent experimental series.

2.8.   Inhibitor experiments in *C. reinhardtii*

To understand the role of NADPH-oxidase dependent oxidative burst stress, the inhibitor diphenyl iodonium (DPI) (2 µM as final concentration in experiment, Sigma-Aldrich, Germany) and the general antioxidant ascorbic acid (5 mM as final concentration in experiment, Sigma-Aldrich, Germany) were added 30 min before the pulse treatment (at 30 h after subcultivation). Different concentrations of DPI and ascorbic acid already been tested in the preparatory experiments, and the concentrations we selected in our study did not cause adverse effects on cell viability. As negative control, samples with the respective solvent in the same final concentration (0.01 % DMSO for DPI, water in case of ascorbic acid) were prepared and processed in the same manner.

To assess the effect of auxins on proliferation of *C. reinhardtii*, the natural auxin indolyl-3-acetic acid (IAA, Fluka, Buchs; Switzerland), along with the artificial auxins 1-naphthalene acetic acid (NAA, Sigma-Aldrich, Neu-Ulm; Germany), and 2,4-dichlorophenoxyacetic acid (2,4-D Sigma-Aldrich, Neu-Ulm; Germany) were added at the time of subcultivation in a final concentration of 10 µM. To probe a potential effect of natural auxin (IAA) on the palmella formation induced by nsPEFs, 10 µM of IAA were added to the cells 30 min prior to the pulse treatment (at 30 h after subcultivation). And the frequency of palmella formation was quantified under the ApoTome microscope (AxioImager Z.1; Zeiss, Germany) using a 63× oil immersion objective. At least 1,500 cells were determined for each measurement. Data represent mean values and standard errors from three independent experimental series.

2.9. Quantification of astaxanthin and cell diameter of *H. pluvialis*

Astaxanthin content and cell diameter was analyzed by software Image J. One RGB image of cell morphology was acquired by Axioskop microscope (Axioskop 2 FS; Zeiss, Germany) with a digital camera (AxioCam color) and exported into ".tif" format with the AxioVision (Rel. 4.8) software. For astaxanthin content quantification, the color of the RGB image was first inverted into purple by the function of Edit of Image J software, and then the purple color image was split into green, red and blue channels. Due to the green channel represented the red astaxanthin signal, and the red channel was for the green chlorophyll signal, by subtracting the green and red channels, a black and white image was obtained and the signal was corresponding to the pixel intensity of astaxanthin in each cell. At last, the integrated density of cells was quantified in the measuring circle. The individual measurement was stored in a list that is in a different window, and the number of the column major/minor give the diameter of the cell, and the column "IntDen" give the intensity pixel of astaxanthin. The results represent mean values of at least 500 cells per each data point and standard errors of three independent experimental series.

2.10. Salt stress trigger astaxanthin biosynthesis

To determine the relationship between the gene activity and the astaxanthin accumulation, we used salt stress to stimulate astaxanthin biosynthesis. 5 days of *H. pluvialis* were treated with 100 mM and 200 mM NaCl as final concentration, separately. And the cell mortality, MDA content, cell diameter, astaxanthin content and the relative gene expression of *psy*, *crtR-b* and *bkt 1* were quantified at 8, 24, 48, 72 and 96 h after NaCl treatment. Data represent mean values and standard errors from three independent experimental series.

2.11. Gene expression during astaxanthin biosynthesis of *H. pluvialis*

2.11.1. RNA isolation and cDNA synthesis

Aliquots of 4 ml cell suspensions were harvested and the supernatant was removed after centrifugation at 10,000×g for 4 min, then, samples were shock-frozen in liquid nitrogen immediately. One sterilized steel bead was added and the sample was homogenized twice by a Tissuelyser (Qiagen, Retsch, Germany) at 18 Hz for 30 seconds. The total RNA was isolated using the innuPREP Plant RNA Kit (analytikjena, Jena, Germany) according to the manufacturer's protocol. And the RNA concentration was quantified by Biophotometer (D30, Eppendorf, Germany).

The mRNA was transcribed into cDNA by using the M-MuL V RTase cDNA Synthesis Kit (New England BioLabs; Frankfurt am Main, Germany) following the manufacturer's instructions. cDNA was synthesized by two-step reverse transcription methods in 20 μl reaction system, and carried out by Primus 96 advanced[®] PCR thermal cycler (PEQLAB Biotechnologie GmbH, Germany). Step one: each sample used 1 μg RNA as template and fully mixed with 2 μl of Oligo dT, 1 μl of dNTPs (10 mM) and 13 μl of nuclease-free water. Then, the mixed sample was incubated at 70 °C for 5 min by PCR program. Step two: after the incubation from step one, the mixed sample was added with 2 μl of 10× Reverse Transcript (RT) buffer, 1 μl of RNAse inhibitor and 1 μl of M-MulV RTase. After fully mix, all the samples were transferred back to the PCR system and incubated at 42 °C for 1 h and at 90 °C for 10 min. Finally, the cDNA was 1:10 dilution by nuclease-free water and storage under 20 °C for further measurement.

2.11.2. Quantification of *psy, crtR-b* and *bkt1* by quantitative RT-PCR

To investigate the relative mRNA transcript level of gene *psy, crtR-b* and *bkt 1* after nsPEFs and NaCl treatment, the quantitative real-time PCR (qRT-PCR) was performed. The sequences of each gene were shown in **Table 2.5**. The qRT-PCR products were quantified by CFX96 Touch™ Real-Time PCR Detection System (Bio-Rad, Germany). In 20 µl reaction system, the PCR contained 4 µl of 1× GoTaq colorless buffer, 11.75 µl of nuclease-free water, 0.4 µl of dNTPs (10 mM), 0.4 µl of each primer (10 mM), 1 µl of $MgCl_2$ (50 mM), 0.1 µl of GoTaq polymerase (Promega, Mannheim, Germany), 0.95 µl 10×SYBR green (Invitrogen, Darmstadt, Germany) and 1 µl of 1:10 dilution cDNA template. The amplification conditions were 95 °C /3 min, followed by 39 cycles of 95 °C /15 s and 63 °C /40 s. The blank reactions were amplified by using nuclease-free water instead of cDNA template. *Actin* was used as a housekeeping reference (Huang *et al.*, 2006), the C_t values from each measurement were normalized to the respective value of *actin* as internal standard, and the relative expression level of each gene were normalized to control$_{18 h}$. The final result was expressed as $2^{-\Delta\Delta C_{t(X)}}$.

Table 2.5 Primers and literature references used for qRT-PCR

Name	GenBank accession No.	Primer sequence (5'-3')	Reference
psy	AF305430	F: AGGGGATGCGGATGGATTTGC	(Steinbrenner&Linden, 2001)
		R: AGTCATCAGGCCAACAGTGCC	
crtR-b	AF162276	F: TGCTGCTACCACGATGCTGT	(Steinbrenner&Sandmann, 2006)
		R: CATGCAGGCAGACTTTGGGC	
bkt 1	GU143688	F: CACAGCTAGACGGATGCAGCT	(Lu *et al.*, 2010)
		R: GCCTGCAACCTCCTTCTCCTT	
actin		F: GCGGGACATCAAGGAGAAGCT	(Huang *et al.*, 2006)
		R: TCGTAGTGCTTCTCCAGTGCC	

2.12. Statistical analyses

All experiments were performed in three independent experimental series. The data represent in mean values and standard errors. The results of three replicates were carried out using Microsoft Office Excel Software (version 2010). The statistic test presented in * P=0.05, **P=0.01.

3. Results

In this chapter, the results from this study can be divided into two parts. In the first part, we investigated the role of oxidative burst for the developmental cellular responses induced by nsPEF in *C. reinhardtii*. A short-term and long-term cellular response to nsPEFs was determined. In the study of the long-term response, a specific NADPH oxidase RboH inhibitor DPI and unspecific ROS scavenger Asc were used to manipulate the oxidative burst appeared at 5 days later triggered by nsPEFs. Then we used salt stress to mimic the generation of oxidative burst and osmotic stress in *C. reinhardtii* to induce the formation of palmella stage. At last, we used both natural and artificial auxin to manipulate the formation of palmella stage generated by nsPEFs. In the second part, we applied nsPEFs on another algae *H. pluvialis*. To dissect whether nsPEFs could stir the cellular responses of *H. pluvialis* and trigger the astaxanthin biosynthesis prior to the formation by itself. A long-term response and the astaxanthin accumulation in *H. pluvialis* were investigated. Salt was used as stress factor to trigger the astaxanthin biosynthesis, and the gene expression level during the astaxanthin biosynthesis was quantified, and the differences of cell response between salt and nsPEFs stimulation were compared.

3.1. NsPEFs trigger cell differentiation in *C. reinhardtii*

3.1.1. Short-term response of *C. reinhardtii* to nsPEFs

To investigate the short-term response of *C. reinhardtii* to nsPEFs, cells were subjected to pulse treatment at day 4 after subcultivation. Cell membrane permeabilization, cell diameter, and MDA content as measure for lipid peroxidation were quantified before and over the first two hours after pulse treatment (**Fig. 3.1**). When measuring short-term responses, 0 min indicated the condition prior to pulse treatment, and 4 min the earliest possible time point

after the treatment, because the 30 ml of suspension required 4 min to pass the treatment chamber.
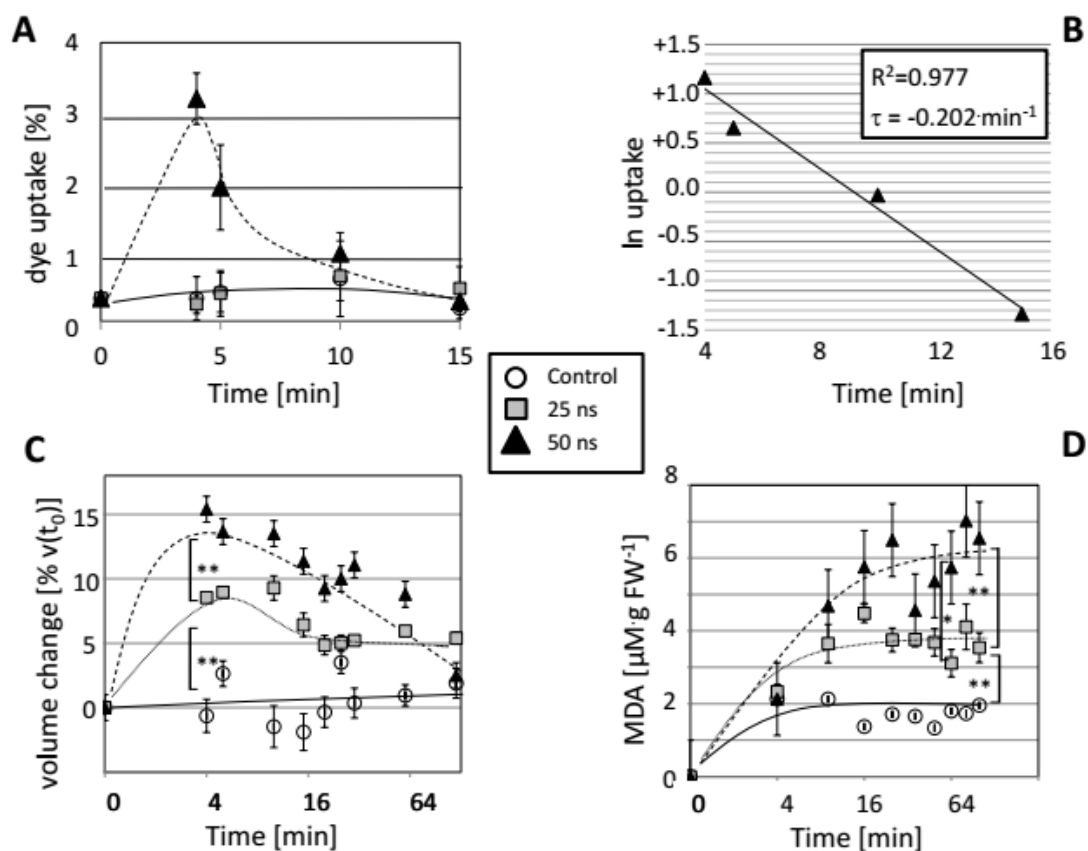
Figure 3.1: Short-term response of *C. reinhardtii* to pulse treatment. **A** Transient membrane permeabilization measured as percentage of cells taking up the membrane-impermeable dye Evan's Blue added at the respective time after pulsing. A sham sample (control) was compared to a pulse treatment with a pulse duration of 25 ns (grey squares), and a treatment with 50 ns (black triangles). **B** Determination of the time constant for resealing by plotting the natural logarithm of uptake values for the 50 ns treatment and determining a linear regression line. The slope of this line gives an estimate for the time constant of resealing of the membrane, the regression coefficient gives an estimate for the validity of the approximation by a model assuming a first-order kinetics of resealing. **C** Time course of volume change (in % of start volume) in response to nsPEFs treatment. **D** Time course of lipid peroxidation in response to nsPEFs treatment. Data represent mean values, error bars s_e of three independent experimental replications.

Brackets indicate significant differences (* *P*=0.05, ** *P*=0.01).

Transient membrane permeabilization was measured as percentage of cells taking up the membrane-impermeable dye Evan's Blue added at the respective time after pulsing. In comparison to the control, a treatment with a pulse duration of 25 ns did not cause an obvious change in membrane permeability (**Fig. 3.1A**). In contrast, for a pulse duration of 50 ns, about 3 % of cells took up the Evan's Blue if the dye was added 5 min after pulsing treatment (which was the earliest measurable time point due to the delay caused by the handling of the samples). If the dye was added later, uptake was found to decrease until the membrane had become again completely tight 15 min after the pulse. To determine the time constant for this membrane resealing after the 50 ns pulsing, a first-order kinetics was assumed, such that the natural logarithms of the values could be approximated by linear regression (**Fig. 3.1B**). From the slope of this line, the time constant was estimated to be around -0.2 min^{-1}, and since the regression coefficient was very close to unity, this approximation by a model assuming a first-order kinetics of resealing was found to be valid.

To verify, whether this transient increase of membrane permeability would result in a temporary swelling of the cell, we followed cell diameter over the first two hours after pulsing (**Fig. 3.1C**). Whereas, in control samples, the average volume of cells showed only minor fluctuations during the experiment, both, pulsing at 25 ns and 50 ns, produced a rapid increase of volume, followed by a gradual decrease. This transient swelling was more pronounced for the 50 ns pulse, but also observed for the 25 ns pulse. Thus, the volume increase was found to monitor membrane permeability more sensitively as the Evan's Blue exclusion assay.

To find out, whether the transient permeabilization of the membrane would result in increased lipid peroxidation, we measured the content of MDA as

stable end product of lipid conversion (**Fig. 3.1D**). Again, both treatments, pulsing at 25 ns and 50 ns, respectively, caused a rapid increase of MDA levels that reached a plateau from around 15 min after the pulse. This plateau was significantly higher for pulsing at 50 ns as compared to 25 ns. In summary, *C. reinhardtii* responds to nsPEFs by a rapid and transient increase of membrane permeability, accompanied by a transient volume increase, and a somewhat slower lipid peroxidation. These responses become more pronounced when the input energy is doubled by increasing the duration of the pulse from 25 ns to 50 ns.

3.1.2. Long-term response of *C. reinhardtii* to nsPEFs

The elevated membrane permeability observed immediately after the nsPEFs treatment was found to be transient with restoration of the original situation within 2 h (**Figs. 3.1A, C**). In contrast, the stimulated lipid peroxidation as recorded by MDA remained on a plateau over the tested time interval (**Fig. 3.1D**). This led to the question, whether the short pulse treatment would cause any long-term response in *C. reinhardtii*. We therefore administered a nsPEFs treatment at 30 h after subcultivation, i.e. at the time of maximal proliferation activity. After pulsing, all cell suspensions returned to the incubator and cultivation continued till day 7, while optical density as measure of culture growth (OD_{750}), cell diameter, cell number, and MDA content were measured every day to detect potential long-term changes in response to the nsPEFs treatment (**Fig. 3.2**).

In fact, already from 18 h after the pulse treatment, the OD_{750} in both treatments, i.e. pulsing with 25 ns and 50 ns, was significant decreased compared to control, reaching a plateau that was significantly lower around two days earlier than in the wild type (**Fig. 3.2A**). Secondly, while the cell diameter in the control decreased sharply in consequence of cell division after 1 day of subcultivation and remained at this lower level till day 3, this drop was

42

stopped immediately after pulsing, such that cell diameters in both treatments, i.e. pulsing with 25 ns and 50 ns, remained larger than those of the controls until day 4 of cultivation (**Fig. 3.2B**).
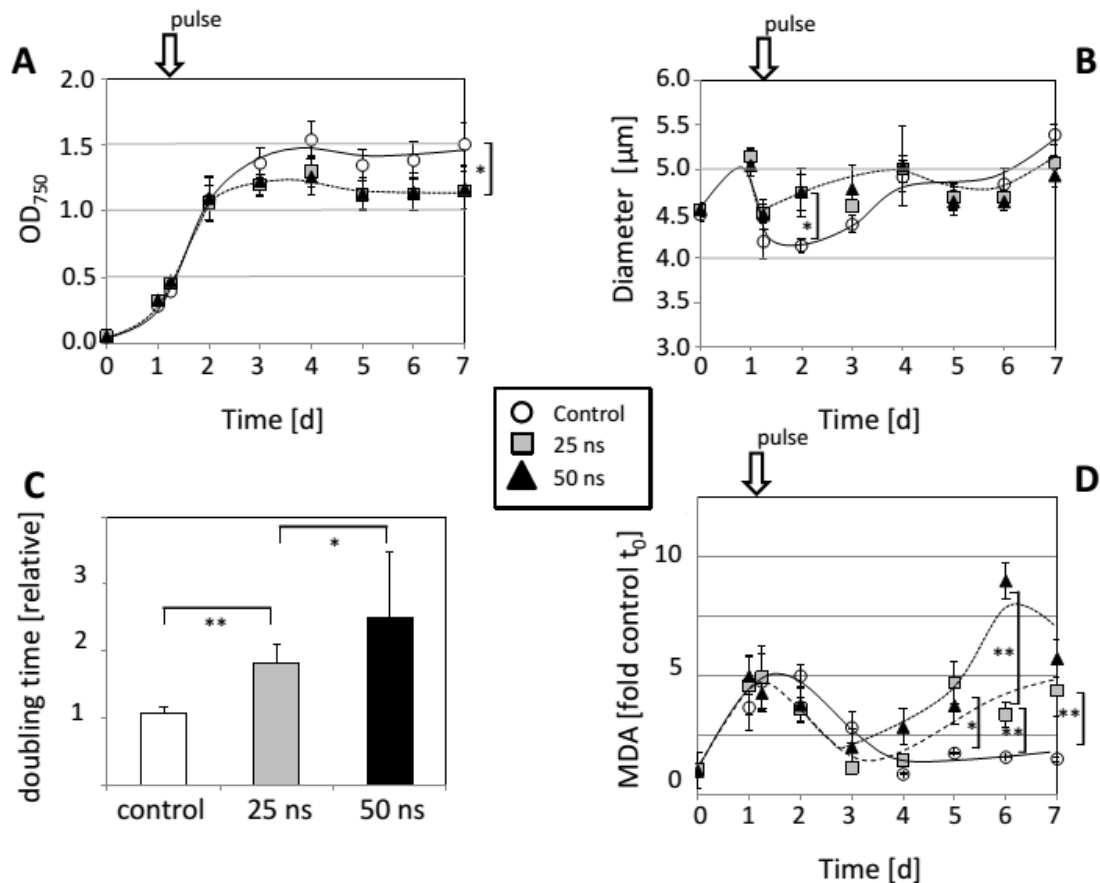
Figure 3.2: Long-term response of *C. reinhardtii* to pulse treatment. **A** Time course of optical density at 750 nm as measure for cell number. **B** Time course of cell diameter as measure for cell expansion. **C** Effect of nsPEFs treatment on doubling time as measure for cell cycle duration. **D** Time course of lipid peroxidation. Brackets indicate significant differences (* P=0.05, ** P=0.01).

Since optical density depends on both cell number and cell size, cell numbers were determined directly by means of a cell counter, and from these numbers, mean cell cycle durations could be derived based on a model of exponential proliferation (**Fig. 3.2C**). These estimated doubling times were significantly increased by the nsPEFs treatment. Although both pulse treatments, with

durations of 25 ns and 50 ns, could slow down the cell cycle compared to the control, the effect caused by pulse durations of 50 ns was significantly stronger than that for 25 ns.

Since nsPEFs had produced an increase of MDA that was persistent over the tested first two hours (**Fig. 3.1D**), we followed MDA content over the entire cultivation cycle. In the control, MDA levels increased during the proliferation phase and then decreased, when the culture passed from proliferation into cell expansion, and then remained low throughout the rest of the cultivation cycle (**Fig. 3.2D**). The pattern observed after pulsing at 25 ns or 50 ns, respectively, was initially very similar: a transient increase at day 2, followed by a decrease back to the initial levels prior to proliferation without significant differences to the control. However, whereas MDA levels remained low in the control from day 3, in the pulsed samples, MDA levels rose again reaching a second peak on day 6. This peak was substantial, especially for pulsing at 50 ns. Again, the amplitude of this long-term increase of MDA indicative of elevated lipid peroxidation was proportional to the input energy (caused by the difference in pulse duration). Thus, nsPEFs cause a persistent long-term increase in lipid peroxidation in *C. reinhardtii* although the membrane permeability caused by the pulse is transient.

3.1.3. The persistent response of lipid peroxidation to nsPEFs can be blocked by DPI

To get insight into the molecular mechanisms underlying the long-term response of lipid peroxidation in response to nsPEFs, 2 µM of DPI or 5 mM of Asc as final concentration, respectively, were added 30 min before administering the pulse at the usual time, 30 h after subcultivation. Cell diameter, cell number, and MDA content were measured on day 5 after subcultivation, i.e. at a time point, where the long-term response of lipid

peroxidation was increasing and had not yet reached saturation.

DPI as an inhibitor of the NADPH oxidase RboH clearly eliminated the production of MDA to the level observed in untreated controls on day 5 (**Fig. 3.3A**). In contrast, ascorbic acid, used as unspecific ROS scavenger, failed to mitigate the enhanced lipid peroxidation caused by the pulsing treatment (**Fig. 3.3B**), and in unpulsed controls even stimulated the MDA levels.

The long-term effect of DPI (given 30 h after subcultivation) on cell expansion was different: whereas cell diameter at day 5 was significantly inhibited in the unpulsed control (**Fig. 3.3C**), such an inhibition was not observed in any of the pulsed samples. For cell number scored at day 5 of cultivation, the inhibitor (administered 30 h after subcultivation) caused a reduction to comparable levels for both control and pulsed samples, irrespective of the fact that the cell density was already significantly reduced by the pulsing even without DPI (**Fig. 3.3D**).
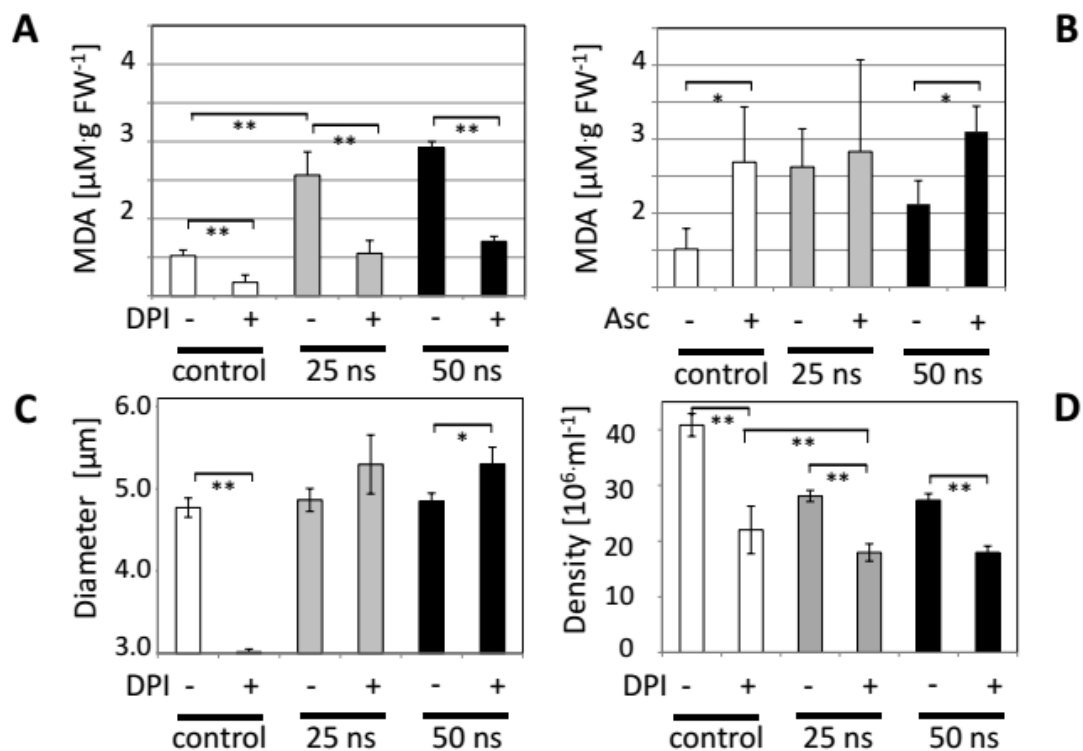
Figure 3.3: Role of reactive oxygen species for the long-term response to pulse treatment.

A Influence of DPI as inhibitor of the NADPH oxidase RboH was measured on the long-term response of lipid peroxidation. **B** Asc as general ROS scavenger was used as control for lipid peroxidation. **C** Cell diameter. **D** Cell density measured at day 5. DPI (2 µM) or Asc (5 mM) was added 30 min prior to administering the nsPEFs treatment at 30 h. Brackets indicate significant differences (* P=0.05, ** P=0.01).

In addition, we observed a developmental response to nsPEFs (**Fig. 3.4A**). After pulsing at the 30 h of subcultivation, the frequency of palmella stage formation observed on day 5 of cultivation was significantly increased (**Fig. 3.4A**). Whereas the 25 ns treatment produced an increase by about 10 % compared to the control, the 50 ns treatment yielded even 20 % more palmella stages than the control (**Fig. 3.4B**).
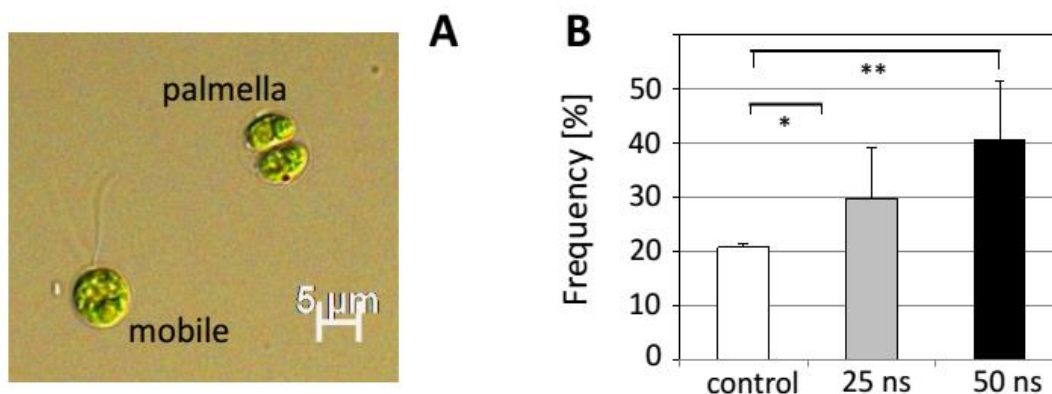
Figure 3.4: Induction of palmella stage in response to pulse treatment. **A** Representative cells for the nsPEFs treatment. **B** Frequency of palmella stages at day 5 of the culture cycle under control condition, and following a nsPEFs treatment with 25 ns or 50 ns, administered at 30 h. Brackets indicate significant differences (* P=0.05, ** P=0.01).

3.1.4. Long-term response to salt stress

Our previous experiments had shown an increase in the content of MDA indicative of stimulated lipid peroxidation several days after a nsPEFs treatment. This was accompanied by an increased frequency of palmella

stages. To investigate, whether this developmental response was linked with lipid peroxidation, we tested the influence of salt stress as independent stress factor known to stimulate lipid peroxidation. Cells were cultivated in the presence of different concentrations of NaCl, and OD_{750} was followed over 7 days, while MDA content and the frequency of palmella stage cells were determined on day 4.
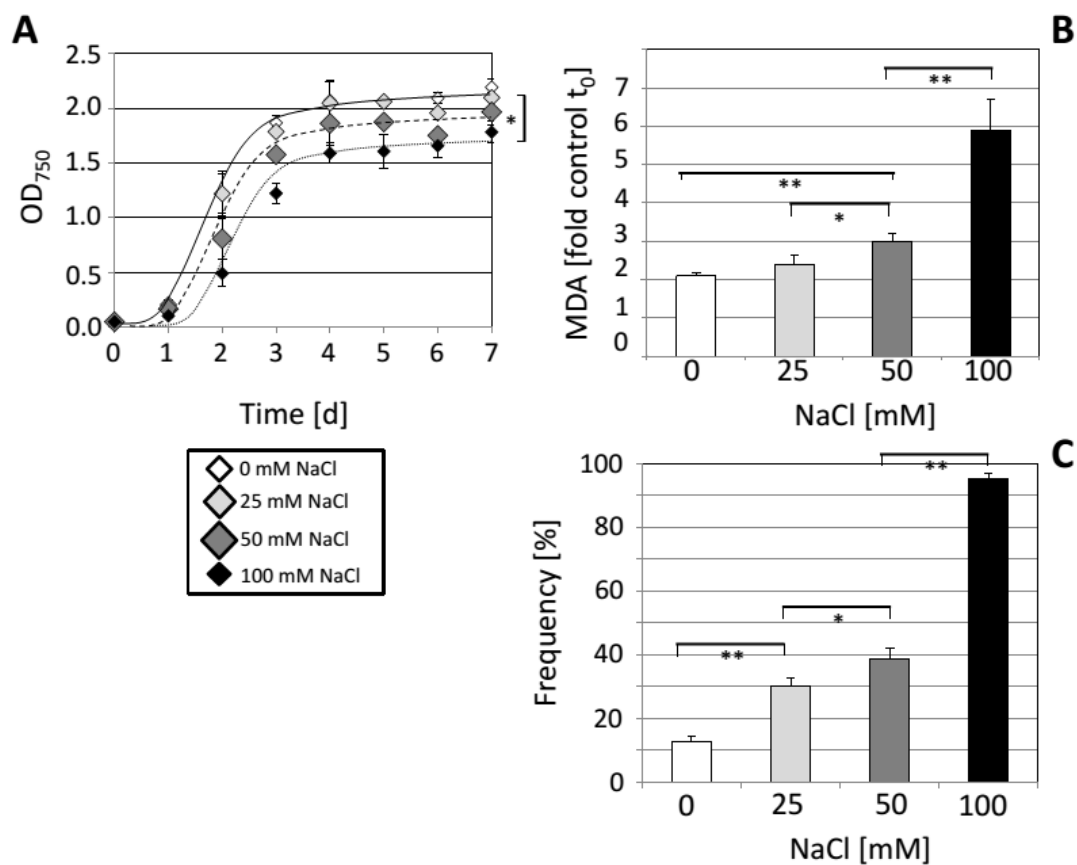
Figure 3.5: Long-term response to salt stress. **A** Time course of optical density at 750 nm as measure for cell number in presence of different concentrations of NaCl. **B** Lipid peroxidation measured at the onset of stationary phase at day 4. **C** Frequency of palmella stages at the onset of stationary phase at day 4. Data represent mean values, error bars s_e of three independent experimental replications. Brackets indicate significant differences (* P=0.05, ** P=0.01).

The results show that cells were able to grow for all NaCl treatments, even at

the highest tested concentration (100 mM NaCl). However, the lag phase was prolonged with increasing concentration of salt, whereas the transition to the stationary phase invariable occurred at day 4. As a result, the final OD_{750} was progressively reduced as the concentration of NaCl increased (**Fig. 3.5A**). In parallel, at the onset of stationary phase at day 4, both MDA levels and the incidence of palmella stages increased, when the concentration of NaCl was raised (**Figs. 3.5B, C**). These data show that the transition into the palmella stage was promoted also for a situation, when lipid peroxidation (as monitored by MDA) was stimulated through a stress factor different from nsPEFs.

3.1.5. Influence of natural and artificial auxins

Since the formation of the palmella stages occurred at the transition to the stationary phase, and since this transition can be modulated by the phytohormone auxin (IAA) in higher plant cells (Campanoni, 2005), we tested, whether the responses of *C. reinhardtii* to nsPEFs might be modulated by auxin as well. To investigate, whether these algal cells are responsive to auxins at all, in a first experiment, the natural auxin IAA was added, in parallel to the artificial auxins NAA and 2,4-D, and the OD_{750} was followed for each auxin treatment over the cultivation cycle of 7 days.

Compared to the control cultivated in the absence of auxin, IAA caused a significant reduction during the cycling phase of the culture, whereas it increased the OD_{750} during the phase of cell expansion in the second stage of the culture (**Fig. 3.6A**). The artificial auxin NAA strongly decreased OD_{750} at the beginning of the cycling phase, but had a slightly increasing effect throughout the subsequent stage (from day 2 to day 7), indicative for a block of cell proliferation and a stimulation of cell expansion. For the artificial auxin 2,4-D as well, an initial decrease was followed by a subsequent increase of OD_{750}. However, the time course was different: the inhibition of cycling was more persistent, and the increase of cell expansion was transient, indicative of

48

a delayed transition into cell expansion. These experiments show that both natural and artificial auxins can modulate the developmental sequence of *C. reinhardtii*, whereby the effect of the two artificial auxins on the cycling and the expansion phase of the culture differ, as it also has been reported for cells from higher plants. It can therefore be concluded that *C. reinhardtii* is endowed with a functional system to sense and process auxin as a signal. We therefore wondered, whether the modulation of development by auxin might be able to interfere with the transition into the palmella stage. In controls, the formation of palmella stages at day 5 was completely suppressed by adding IAA at the time, where the pulse was administered (**Fig. 3.6B**). However, IAA could not suppressed the palmella stages formation which stimulated by the nsPEFs treatment, indicating that the process triggered by the nsPEFs treatment at 30 h, had become irreversible at the time, when auxin was added.
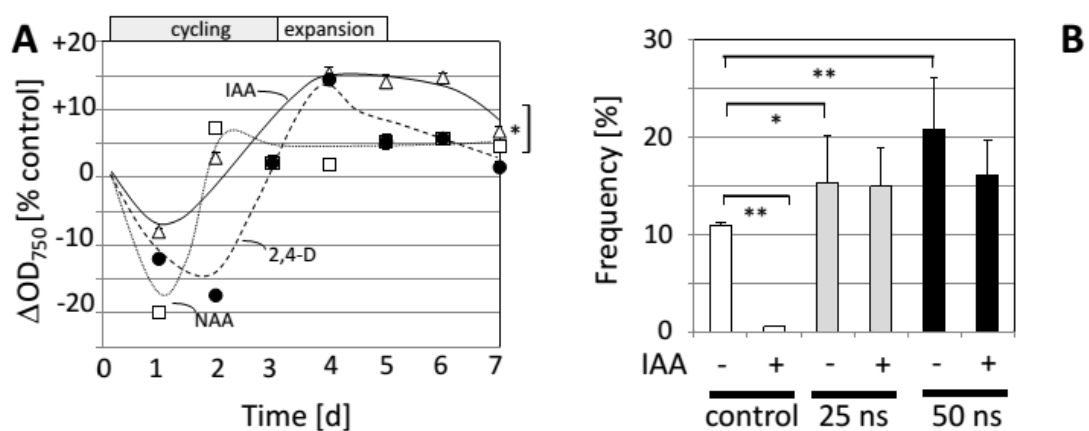
Figure 3.6: Influence of natural and artificial auxins. **A** Time course of modulation of optical density at 750 nm (plotted as differential with the value observed in the untreated control) caused by 10 µM of the natural auxin IAA, the artificial auxin NAA, or 2,4-D added at subcultivation. **B** Effect of natural auxin (IAA) on the frequency of palmella stages at day 5 of the culture cycle under control condition, and following a nsPEFs treatment with 25 ns or 50 ns, administered at 30 h. Data represent mean values, error bars s_e of three independent experimental replications. Brackets indicate significant differences (* *P*=0.05,

** *P*=0.01).

3.2.   Long-term cellular response of *H. pluvialis* to nsPEFs

3.2.1. Cellular response of *H. pluvialis* to nsPEFs

To get insight into the long-term response of *H. pluvialis* to nsPEFs, 5 days old cells were treated with 25 ns (2 $J \cdot g^{-1}$) and 50 ns (4 $J \cdot g^{-1}$) separately. And the cell mortality, cell diameter, astaxanthin content (**Fig. 3.7**) and the relative transcript level of gene *psy, crtR-b* and *bkt 1* (**Fig. 3.8**) were determined at 18, 24, 48, 72 and 96 h after pulse treatment.

Cell mortality was measured as the percentage of the dead cells stained by membrane-impermeable dye Evan's Blue. In control, the cell mortality was below 3 % during the whole test, but nsPEFs could induce a seriously cell mortality (**Fig. 3.7A**) to *H. pluvialis*. At 18 h after pulsing, the cell mortality in 50 ns already reached up to 15 % and about twice higher than in 25 ns. And this situation maintained until the 48 h after pulsing, then a sharp increase in both 25 ns and 50 ns was observed, and the cell morality finally come to about 19 % at 96 h in both pulsing treatment.

The cell diameter and astaxanthin content were analyzed by Image J software, and the results were represented by the percentage of increase to $control_{18h}$ (**Fig. 3.7B, C**). 18 h after nsPEFs treatment, the astaxanthin content increased about 10 % and 16 % in response to 25 ns and 50 ns, respectively (**Fig. 3.7B**). For 50 ns treatment, the astaxanthin continue increased and maintained 15 % higher than $control_{48h}$ at 48 h, and then gradually decreased to the same level of control. However, there was no obvious stimulation of astaxanthin accumulation under 25 ns treatment. About the change in cell volume, the diameter of *H. pluvialis* enlarged to 6 % and 4 % in response to 25 ns and 50 ns at 18 h separately (**Fig. 3.7 C**), and this enlargement remained until 48 h in both 25 ns and 50 ns treatments, then a further increased at 72 h and finally

50

maintained at 5 % higher than $control_{96h}$ for both 25 ns and 50 ns treatment.
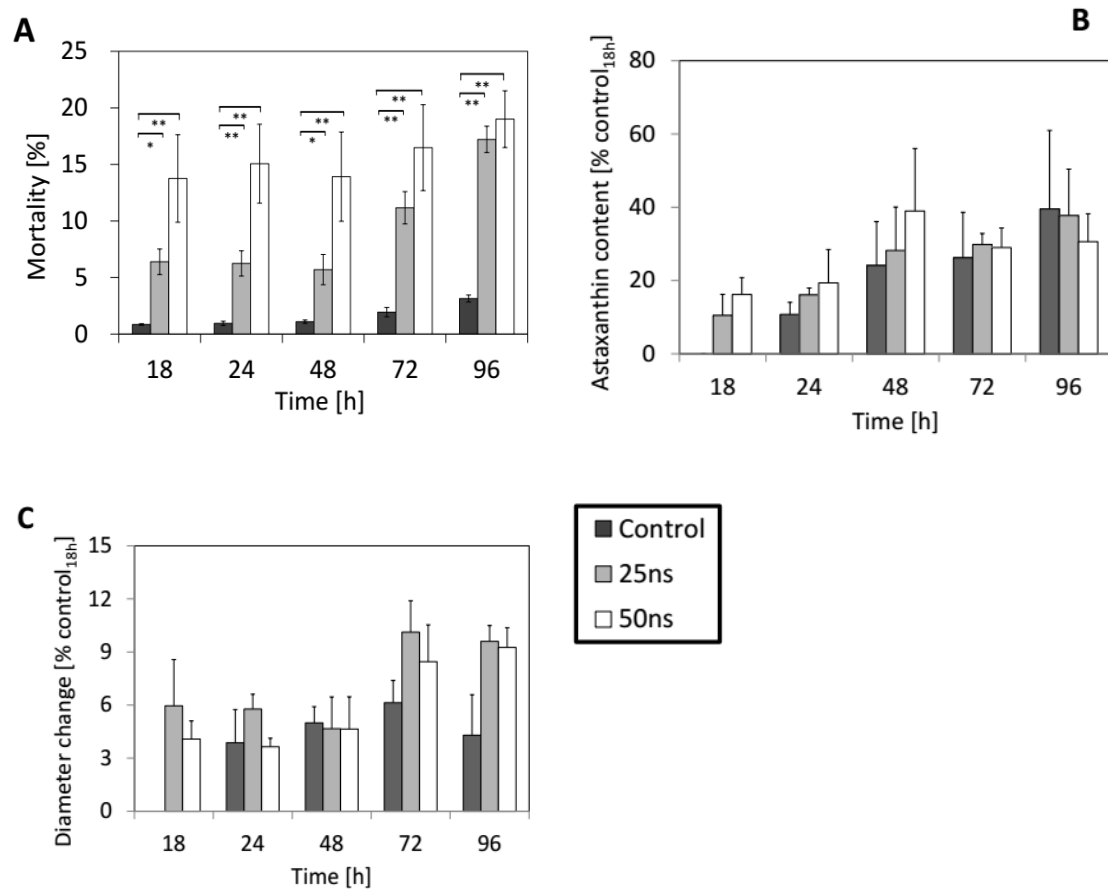
Figure 3.7: Long-term response of *H. pluvialis* to nsPEFs. **A** Time course of cell mortality measured by the uptake of membrane-impermeable dye Evan's Blue. **B** Time course of astaxanthin content (increase in % of $control_{18h}$) in response to nsPEFs. **C** Time course of cell diameter change (increase in % of $control_{18h}$) as measure for cell enlargement. Brackets indicate significant differences (* $P=0.05$, ** $P=0.01$).

Gene *psy*, *crtR-b* and *bkt 1* are three important genes involved in the astaxanthin biosynthesis pathway. The gene expression was quantified by qRT-PCR, and the relative transcript level of each gene was normalized to $control_{18h}$.

The result showed that, nsPEFs was able to stimulate the gene expression of *psy*, *crtR-b* and *bkt 1* in transcript level, but the distribution was different between 25 ns and 50 ns treatment. Compared to the mRNA amount in control,

genes *psy* and *bkt 1* were firstly increased at 48 h by 25 ns treatment, and then gradually decreased (**Figs. 3.7A, C**). While for gene *crtR-b*, the peak transcript level of mRNA appeared at 24 h after 25 ns treatment, and then, the level dramatically decreased in compare to control (**Fig. 3.7B**). However, for 50 ns treatment, the peak transcript level of *psy, crtR-b* and *bkt 1* were all postponed to 72 h (**Fig. 3.7**).
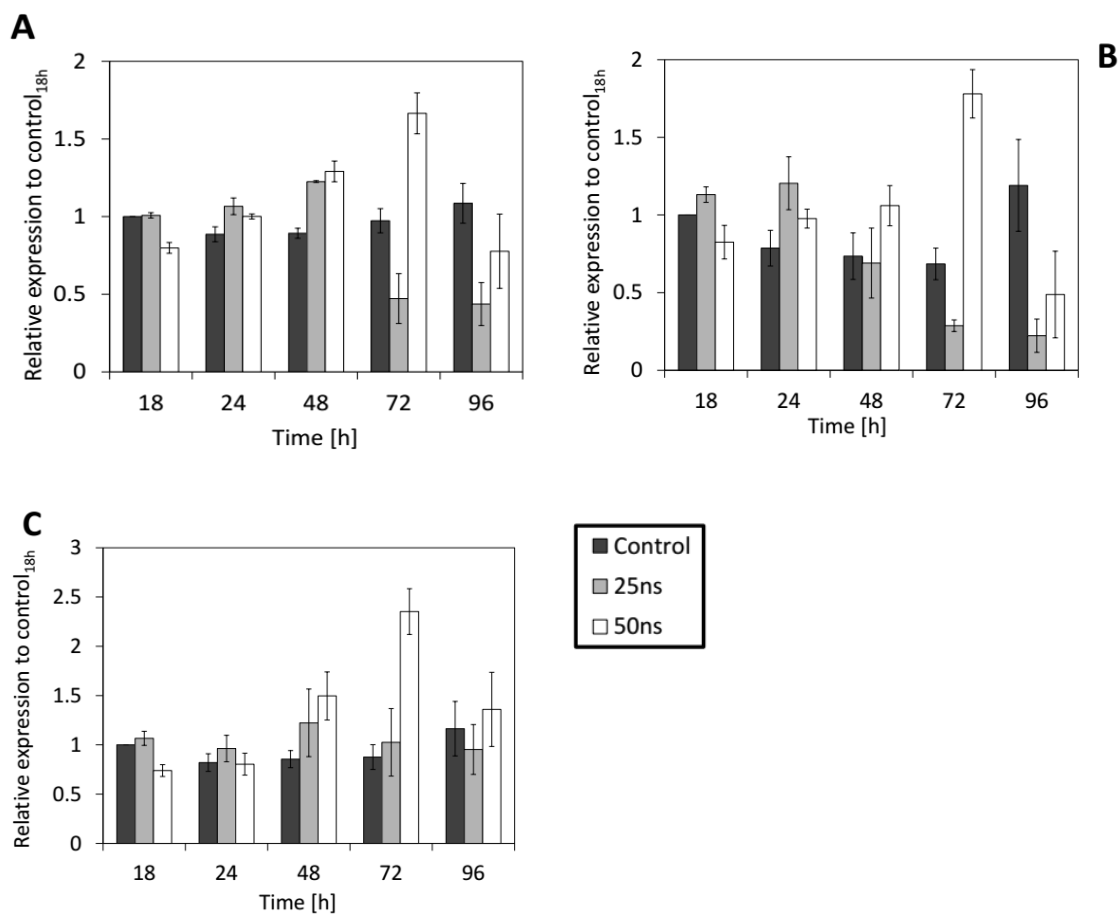
Figure 3.8: Time course of relative gene expression in response to nsPEFs. **A** *psy*. **B** *crtR-b*. **C** *bkt 1*. The relative gene expression was presented in normalized to control$_{18h}$.

3.2.2. Salt stress induced the astaxanthin accumulation in *H. pluvialis*

As nsPEFs could stimulate the gene expression of *psy*, *crtR-b* and *bkt 1* on transcript level but slightly astaxanthin accumulation, we use salt stress to

stimulate the astaxanthin biosynthesis in *H. pluvialis*, and to further compare the cell responses between nsPEFs and abiotic stress treatment.

In the study of salt stress stimulation, we used 5 days old *H. pluvialis* and treated with 100 mM and 200 mM NaCl as final experiment concentration separately. To investigate a long-term cell response to salt stress, the cell mortality, MDA content, cell diameter, astaxanthin content (**Fig. 3.9**) and the relative gene expression of *psy*, *crtR-b* and *bkt 1* (**Fig. 3.10**) were determined at 8, 24, 48, 72 and 96 h after the salt treatment.

After the addition of different concentrations of NaCl, *H. pluvialis* could switch from green vegetative stage to the red cyst stage immediately. In comparison to the control, the cell diameter had no obvious change in 200 mM NaCl, but there was slightly decrease in 100 mM NaCl (**Fig. 3.9A**). However, 200 mM NaCl could trigger the astaxanthin accumulation after 8 h, while there was slightly decreased of astaxanthin content after 100 mM NaCl treatment compared to control (**Fig. 3.9B**). By determine the MDA content, 100 mM NaCl showed no obvious stimulation on the oxidative burst in *H. pluvialis*. But after the addition of 200 mM NaCl, the MDA content was significant increased after 48 h compared to control (**Fig. 3.9C**). Besides, the salt stress also induced a rise in cell mortality (**Fig. 3.9D**), in control, the cell mortality was below 3 % during the test, whereas the mortality immediately increased to about 11 % and 8 % at 8 h after the addition of 100 mM and 200 mM NaCl, respectively. And in 100 mM NaCl treatment, the cell mortality was gradually increased over time and reached up to 26 % at 96 h, while in 200 mM NaCl, the cell mortality dramatically increased after 8 h and finally maintained at 82 % after 96 h.
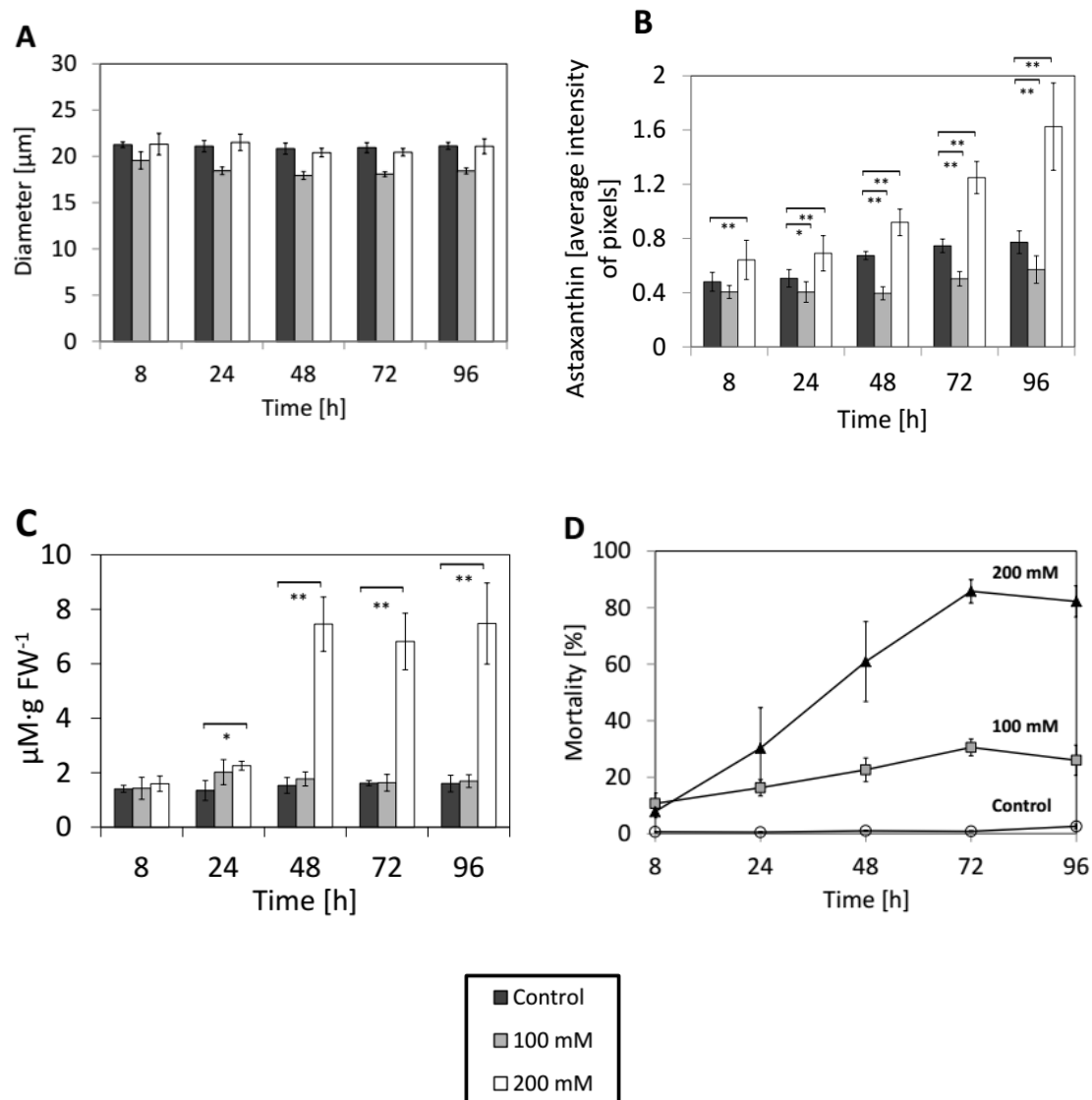
Figure 3.9: Long-term response of *H. pluvialis* to salt stress. **A** Time course of cell diameter measured as cell expansion. **B** Time course of astaxanthin content presented by the average intensity of pixels of astaxanthin signal. **C** Time course of MDA content measured for oxidative burst. **D** Time course of cell mortality measured by the uptake of membrane-impermeable dye Evan's Blue. Brackets indicate significant differences (* P=0.05, ** P=0.01).

As *H. pluvialis* showed obvious cell responses to NaCl stimulation, the relative mRNA expression of *psy*, *crtR-b* and *bkt 1* also presented distinct differences between 100 mM and 200 mM salt stress (**Fig. 3.10**).

In 100 mM NaCl treatment, the transcript level of all three genes were

obviously decreased during 96 h cultivation compared to control (**Figs. 3.10A, B, C**), especially for *psy* and *crtR-b*, the transcript level decreased about 50 % and 81 % in average compared to each control separately within the first 48 h after the addition of NaCl (**Figs. 3.10A, B**), and then, the amount of mRNA was gradually increased but still below their corresponding control until 96 h.
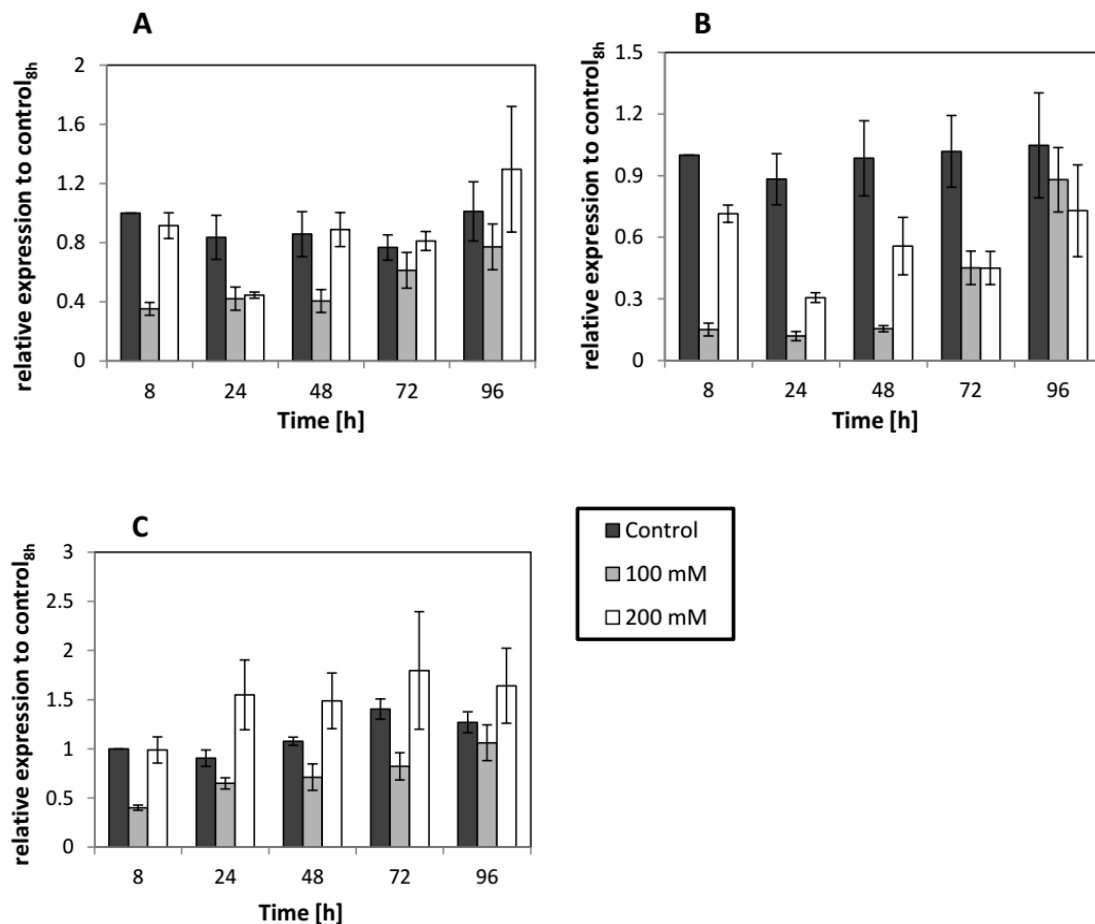
Figure 3.10: Time course of relative gene expression in response to 100 and 200 mM NaCl stress. **A** *psy*. **B** *crtR-b*. **C** *bkt 1*. The relative gene expression was presented in normalized to control$_{18h}$.

However, in 200 mM NaCl treatment, the transcript level were various among *psy*, *crtR-b* and *bkt 1*. Firstly, for gene *psy*, there was no obvious change of expression at 8 h compared to control$_{8h}$, but there was about 39 % decreased at 24 h, and then, the distribution was increased immediately and finally

increase about 29 % than control$_{96h}$ at 96 h (**Fig. 3.10A**). Secondly, the transcript level of *crtR-b* was totally decreased compared to control within 96 h in 200 mM NaCl treatment (**Fig. 3.10B**), but not as serious as in 100 mM treatment, which after 8 h cultivation, the gene expression was only 29 % lower than control$_{8h}$, and the lowest amount appeared at 24 h, which was 58 % lower than control$_{24h}$, and then the mRNA was gradually increased but still 32 % lower than control$_{96h}$ at last. However, the transcript level of gene *bkt 1* was totally induced by 200 mM NaCl (**Fig. 3.10C**). In comparison to control, the expression of *bkt 1* was obviously increased after 24 h, even though the distribution of *bkt 1* in control was also slightly increased after 24 h cultivation, the induction of *bkt 1* by 200 mM NaCl was still 45 % in average higher than the expression level in control after 24 h.

Besides, we also studied a long-term astaxanthin biosynthesis stimulated by other stress factors, including cultivation under red and blue light irradiation, and a long-term salt stress begin with inoculation. And the experiment details and results were shown in **Appendix**.

3.3.   Summary

NsPEFs could generate electroporation on cells and induce a series of cellular responses, but the mechanisms behind this are still far from understood.

In our study, we used microalgae *C. reinhardtii* as our experimental model and treated with nsPEFs. To investigate the cell responses to the stimulation of nsPEFs, a short-term response was studied by treating with 4 days old *C. reinhardtii*, and a long-term response was observed by performing at 30 h after inoculation. In the short-term response, a membrane-impermeable dye Evan's Blue was used as a marker to detect membrane integrity, and we found out that, nsPEFs could generate a transient membrane permeability on *C. reinhardti.* For 50 ns treatment, the membrane permeability was recovered at 15 min after pulsing, whereas for 25 ns, the permeability was instant and undetectable. Besides, nsPEFs also induced a rapid cell swelling and lipid peroxidation, and the responses were increased as the pulse duration doubled from 25 ns to 50 ns. In the long-term responses, we used cell counter to quantify the cell density and diameter, and MDA assay as read out for lipid peroxidation. The results showed that, nsPEFs prolonged the cell division, decreased cell density, stimulated cell expansion by induced the formation of palmella stage, and generate a long-term persistent lipid peroxidation several days later after pulsing. To testify whether the long-term lipid peroxidation induced by nsPEFs was the reason for the formation of palmella stage. On one hand, a NADPH-oxidase RboH inhibitor DPI and ROS scavenger Asc was added at 30 min prior to nsPEFs treatment to block the formation of ROS. On the other hand, salt stress was used to stimulate the generation of ROS. We concluded that, the formation of palmella stage induced by nsPEFs was correlated with this long-term persistent increasing of lipid peroxidation. At last, natural auxin IAA and artificial auxin NAA and 2,4-D was used to modulate palmella stage formation. However, the palmella stage induced by nsPEFs

was irreversible and could not be suppressed by IAA.

Then, we applied nsPEFs on microalgae *H. pluvialis,* to investigate whether the nsPEFs could manipulate gene expression and trigger the astaxanthin biosynthesis in *H. pluvialis*. We performed nsPEFs on 5 days old cell suspensions, the results showed that, nsPEFs induced an increasing of cell mortality and cell enlargement. By quantified the astaxanthin content and gene expression during the astaxanthin biosynthesis, nsPEFs could stimulate a transient response of the expression of *psy, crtR-b* and *bkt 1* on transcript level. However, there was only a slightly and transient astaxanthin accumulation at 48 h after 50 ns treatment, and no obvious accumulation under 25 ns treatment in *H. pluvialis*. Furthermore, we used one stress factor--salt stress to trigger the astaxanthin biosynthesis in 5 days old *H. pluvialis,* the results showed that, 200 mM NaCl could induce a long-term astaxanthin accumulation and cell enlargement than 100 mM NaCl. At mean time, 200 mM NaCl could also leading to a highly cell mortality. The MDA content represented the oxidative burst showed that, 100 mM NaCl could not induced the oxidative burst, but there was a sharp increasing after 48 h in 200 mM NaCl. By comparing the gene expression of *psy, crtR-b* and *bkt 1* between nsPEFs and salt stress, we concluded that, although the gene expression of *psy, crtR-b* and *bkt 1* could in response to both nsPEFs and salt stress, but the expression of gene *psy* and *crtR-b* showed different distributions against the stimulation of nsPEFs and salt stress. However, gene *bkt 1* was induced under both nsPEFs and salt treatment, and maybe played a more competitive role than *psy* and *crtR-b* in astaxanthin biosynthesis.

4. Discussion

To get insight into potential cellular responses to the transient disruption of membrane integrity induced by nsPEFs, we investigated *C. reinhardtii* as ancestral plant cellular model with rapid proliferation, and observed not only immediate cellular changes in consequence of the formation of transient membrane pores, but also long-term responses that were expressed only several days after the pulse treatment. To further study the application of different cell responses triggered by nsPEFs on the induction of valuable compound production by microalgae, we used *H. pluvialis* as another experimental model, which was applied as a potential producer for a highly antioxidant compound called astaxanthin. We performed nsPEFs on *H. pluvialis*, and investigated the astaxanthin biosynthesis during long-term cultivation after the pulse treatment. Furthermore, whether nsPEFs was able to manipulate some key genes expression during the astaxanthin biosynthesis pathway were also involved. At last, salt stress as an abiotic stress factor could trigger the astaxanthin biosynthesis in *H. pluvialis*. We used 100 mM and 200 mM NaCl as final concentration to stimulate *H. pluvialis*, and the differences of astaxanthin biosynthesis in response to nsPEFs and salt stress treatment was compared.

4.1. Electroporation triggers lipid peroxidation

By quantification of MDA, we were able to detect a stimulation of lipid peroxidation after application of a nsPEFs **(Fig. 3.1D)**. This lipid peroxidation developed from within a few minutes after the pulse and persisted for more than an hour. Strong pulsed electrical fields can generate reactive oxygen species even in cell-free medium (Pakhomova *et al.*, 2012) and this might directly lead to the peroxidation of lipids in the membrane. However, the fact that the lipid peroxidation initiates several minutes after the pulse, then

proceeds over more than an hour **(Fig. 3.1D)**, and then remained stable for more than a day **(Fig. 3.2B)**, cannot be explained in terms of ROS generated directly by the electrical field, but strongly indicates a biological, rather than a physical, mechanism. Besides, the permeabilization induced by nsPEFs remains transient though: by measuring the uptake of the membrane impermeable dye Evan's Blue in a pulse-chase set-up, the resealing of the membrane can be followed and shown to follow a first-order kinetics **(Figs. 3.1A, B)**. Even for a pulse duration of 50 ns, the initial leakage has completely dissipated within 10 min. The cellular swelling induced by this transient membrane permeabilization persists a bit longer, but it also remains transient - after a bit more than one hour cells have returned to their initial volume prior to the pulse **(Fig. 3.1C)**. The fact that the cells can readjust their volumes, indicates that the contractile vacuole remains functional and that its activity is not irreversibly impaired by the nsPEFs.

Cellular swelling in response to nsPEFs has been described by several authors and is often explained by a so called colloidal osmotic mechanism (Kinosita&Tsong, 1977), whereby high molecular-weight components of plasma membrane or extracellular matrix are trapped in the cytoplasm in consequence of the electric field. This will create a negative osmotic potential, such that small solutes will enter the cell (Nesin *et al*., 2011). Colloidal osmosis can explain cellular swelling in cells that are growing under isotonic conditions such as mammalian cells. Whether colloidal osmosis occurs in *C. reinhardtii*, remains to be elucidated, but it is not needed here to explain the observed swelling: Like other freshwater protists, *C. reinhardtii* has to cope with a hypotonic medium which means that there is a continuous influx of water into the cell. The contractile vacuole, which is an organelle essential for all non-walled freshwater protists, has to continuously expel the penetrated water. The most straightforward explanation for the slow, but complete readjustment of the original volume over the hour following the pulse treatment is the

ongoing activity of the contractile vacuole. If the contractile vacuole were irreversibly inactivated by the nsPEFs treatment, the cells would burst, because the plasma membrane of cells can maintain integrity only up to an extension of around 3 % (Wolfe *et al.*, 1986).

At a time, when the permeability to Evan's Blue had already vanished, and the transient swelling was already strongly declining, lipid peroxidation, as measured by accumulation of MDA, was still increasing **(Fig. 3.1D)**, and these elevated levels of MDA persisted. Activation of oxidative burst by nsPEFs has been proposed as trigger for biological effects in mammalian cells, in concert with, or possibly even alternatively to, formation of nanopores (Pakhomova *et al.*, 2012). Two mammalian cell lines that differed in their tolerance to nsPEFs treatment, also differed with respect to the accumulation of ROS, which again suggests a biological, rather than a physical mechanism. In our study, the oxidative burst occurs at a time, when the membrane is already resealed, which is consistent with a model, where oxidative burst acts downstream of nanopores formation. A potential mechanism would be the influx of calcium through the nanopores, as proposed from ratiometric measurements of the voltage-sensitive dye annine-6 in tobacco protoplasts challenged by nsPEFs (Flickinger *et al.*, 2010), and patch-clamp studies of tobacco cells challenged by µsPEFs (Wegner *et al.*, 2011). In plant cells, elevation of cytosolic calcium will, through calcium dependent kinases, activate the NADPH oxidase RboH (Dubiella *et al.*, 2013), which would provide a possible mechanism, how the early formation of nanopores would lead to a later oxidative burst. Alternatively, the membrane pores might simply allow the apoplastic superoxide, which is continuously generated by RboH, to leak into the cytosol, which in turn would divert a GTPase of the Rac family towards the activation of RboH, thus producing an autocatalytic loop (Anderberg *et al.*, 2011; Chang *et al.*, 2015). Again, a persistent oxidative burst would then act downstream of pore formation. It should be kept in mind that a temporal sequence and the

existence of a plausible mechanism are still no hard proof for the hypothesis of ROS as second messengers for nsPEFs-dependent pore formation, because, still, the two events could act in parallel with different lag time and, thus, are not necessarily causally linked.

4.2.   Oxidative burst is necessary and sufficient for long-term responses to nsPEFs

Among the primary cellular responses (membrane permeabilization, swelling, lipid peroxidation as readout for oxidative burst), lipid peroxidation was the most persistent, but 1.5 days after the pulse, no physiological imprints of the pulse treatment had remained **(Fig. 3.2)** giving the impression as if the cells had completely reversed to the *status quo ante*. This impression had to be revised, when we followed the development further and observed long-term changes including an induction of cell expansion, a delay of cell division, and a second wave of oxidative burst **(Fig. 3.2)**. This was then followed by the formation of palmella stages **(Fig. 3.4B)**, which in this species represents an adaptive response to osmotic stress (Sahoo&Seckbach, 2015). In other words, the nsPEFs treatment activated a signaling chain that culminates in osmotic adaptation. This leads to two questions: Is the second oxidative burst induced by nsPEFs involved in the formation of palmella stage? Is the primary oxidative burst induced by nsPEFs necessary and sufficient for these developmental responses occurring several days later? To address this question, we added DPI, a specific inhibitor of NADPH oxidases (Cross&Jones, 1986), at 30 min before nsPEFs treatment to block the primary oxidative burst, and we then observed that both long-term oxidative burst generated by nsPEFs were suppressed **(Fig. 3.3A)**, which suggested that the primary oxidative burst is necessary for the long-term effect. We also used ascorbate as a general ROS scavenger which is targeting on hydrogen peroxide and generating the hydroxyl radical (Nappi&Vass, 2000) **(Fig. 3.3B)**, but did not find a suppression

62

indicative of a specific role the ROS generated by RboH that involved in the oxidative burst. Further, we activated RboH by salt treatment (mimicking the natural condition which is encountered by this developmental response, palmella formation), and we found that salt stress could replace the nsPEFs treatment with respect to induction of the long-term oxidative burst and the formation of palmella stages **(Figs. 3.5B, C)**. Thus, an oxidative burst (as that induced by nsPEFs) is necessary and sufficient to elicit long-term responses, such the second wave of oxidative burst, the arrest of cell division, the stimulation of cell expansion, and the formation of palmella stages.

4.3. Palmella formation versus cell division: a role for auxin signaling?

The oxidative burst observed in response to nsPEFs is accompanied by arrested cell proliferation, promoted cell expansion, and, a few days later, by the formation of palmella stages **(Fig. 3.2)**. The same set of phenomena can be induced by salt stress **(Fig. 3.5)**, which represents the natural condition, for which this combination of responses had evolved. In higher plants, the superoxide generated by RboH is not only used as important stress signal, but is also consumed to convey signaling of the important plant hormone auxin. For this reason, in cells of higher plants, superoxide dependent stress responses can be mitigated by addition of auxin (Chang *et al.*, 2015).

Whether the auxin pathway exists in the Green Algae had been a matter of debate over decades. The advent of genomics has allowed to probing for the presence of the respective genes in different taxa. This approach has revealed that *C. reinhardtii* harbors the components for auxin synthesis as well as the pgp1 type of auxin transporters, and components of signaling through the auxin-binding protein 1 (De Smet *et al.*, 2011). In contrast, the PIN-type transporters, and the IAA/AXR-dependent signaling pathway seem to be

absent.

We therefore tested first, whether auxins are active in modulating the development of *C. reinhardtii*. Our results **(Fig. 3.6)** clearly confirmed that both, the proliferation and the expansion phase, were regulated by auxins. However, the functional conservation extended beyond the mere existence of an auxin effect: In higher plants, the artificial auxin NAA stimulates mainly cell expansion, whereas the artificial auxin 2,4-D activates a different signaling pathway activating cell division (Campanoni, 2005). This specific pattern was conserved as well, since the temporal progression of OD_{750} indicated a block of cell proliferation, and a stimulation of cell expansion for NAA, whereas 2,4-D delayed the transition from proliferation into cell expansion. Thus, we conclude that auxin signaling in *C. reinhardtii* is not only present, but also shares functional specificities with the auxin signaling from higher plants. Due to this high degree of conservation, it appeared feasible to assume that also the functional link between RboH and auxin signaling might be conserved. We therefore probed the effect of the natural auxin IAA on palmella formation **(Fig. 3.6B)** and observed that in the absence of nsPEFs, the transition into the palmella stage was strongly suppressed, consistent with the implication of our model that the ground level of superoxide (generated by RboH) was consumed for auxin signaling and therefore was not able to trigger the developmental response (transition into the palmella stage). However, the induction of palmella formation in response to nsPEFs treatment could not be quelled by the preceding application of auxin. It might be possible that the sensitivity of *C. reinhardtii* to auxin is lower than in higher plants, such that higher auxin concentrations might be required to suppress nsPEFs-dependent palmella formation. However, the observation that the concentration of auxin was sufficient to regulate proliferation and expansion, speaks against this possibility. The alternative model would be a second signal, which is deployed by nsPEFs and which is independent from oxidative burst. A possible mechanism might be

other cellular targets of calcium influx through the nanopores. This is feasible, since in addition to the calcium-dependent protein kinases that transduce the calcium signal into an activation of NADPH oxidase (Dubiella *et al.*, 2013), there are numerous other calcium binding proteins that can read out the calcium signal into different downstream responses (for review, see (Kudla *et al.*, 2010)).

4.4.   Astaxanthin biosynthesis in *H. pluvialis* is a transient response to nsPEFs

In our previous study on the cellular responses of *C. reinhardtii* to nsPEFs stimulation, nsPEFs could not only induce a transient membrane permeability and rapid lipid peroxidation, but also generate a long-term persistent oxidative burst which arrest the cell cycle and trigger the formation of palmella stage. Due to nsPEFs could induce a long-lasting stress signal and force *C. reinhardtii* to enter into stress condition. Then, we applied nsPEFs on another microalgae *H. pluvialis*, and the idea of our study is to utilize this long-term signaling induced by nsPEFs as a stress factor to trigger the astaxanthin accumulation in *H. pluvialis*.

After we recalculated the parameters of nsPEFs used for *H. pluvalis*, the input energy of 25 ns and 50 ns were doubled into 2 J·g^{-1} and 4 J·g^{-1} separately compared to the one used for *C. reinhardtii*. Due to the highly input energy applied on *H. pluvialis*, the cells were unable to resistant this stimulation and caused a highly increased in cell mortality (**Fig. 3.7A**). And as the pulse duration increased from 25 ns to 50 ns, the mortality was also significantly enhanced. The reasons for inducing cell mortality were multiple, for *H. pluvialis*, whether it is due to the intense electric energy destroyed the organelles functions, or the oxidative burst induced by nsPEFs causing cell program death, this still need more studies to explore.

There are two main mechanisms of quenching ROS in *H. pluvialis*, one is antioxidative enzymes in green vegetative cells and the initial of astaxanthin accumulation, another strategy is the astaxanthin biosynthesis in red cyst cells, and the latter is suggested as a secondary-defense plan to against a long-term stress stimulation (Kobayashi *et al.*, 1997a; Li *et al.*, 2008). In our study, nsPEFs could initiate the ROS quenching mechanisms in *H. pluvialis*, for which the cell diameter were both enlarged at 18 h after 25 ns and 50 ns treatment separately, and the diameter keep increasing within 96 h, and this morphology change was a sign of *H. pluvialis* to against stress conditions (Kobayashi *et al.*, 1991) (**Fig. 3.7C**). Although the cell morphology enlarged in response to nsPEFs treatment, the astaxanthin content in 25 ns showed no obvious accumulation compared to control (**Fig. 3.7B**), this may be owing to the ROS quenching mechanisms in *H. pluvialis*, which the oxidative burst induced by nsPEFs may already be scavenged before it accumulated and trigger a long-term astaxanthin biosynthesis strategy. However, after we increased the pulse duration to 50 ns, the astaxanthin content showed a transient and slight increased at 48 h after pulsing, which give us a clue that nsPEFs could trigger a short-term response in astaxanthin accumulation in *H. pluvialis* but not efficiency.

As *H. pluvialis* could slightly response the stimulation by nsPEFs in the manner of astaxanthin accumulation. We further explored that whether the cellular responses during the astaxanthin biosynthesis to nsPEFs could down to the gene expression level. PSY, crtR-b and BKT 1 are three important enzymes participating in the pathway of astaxanthin formation, PSY is involved in the formation of β-carotene, while crtR-b and BKT 1 are working together to convert β-carotene into free astaxanthin. According to the results by qRT-PCR, nsPEFs could transient manipulate the gene expression of all three enzymes on transcript level (**Fig. 3.8**). In 25 ns treatment, a peak gene expression of *psy*, *crtR-b* and *bkt 1*appeared within 48 h after pulsing, which revealed a fast

response on astaxanthin biosynthesis in compared to 50 ns treatment (peak gene expression appeared at 72 h). However, 50 ns treatment could induce a higher expression of all three genes than 25 ns did, this may also explain why *H. pluvialis* could accumulate more astaxanthin than 25 ns. And due to the gene expression of *psy, crtR-b* and *bkt 1* also showed a transient induction in response to nsPEFs, this may be the reason for the transient increased in astaxanthin accumulation in 50 ns treatment.

Although nsPEFs could generate oxidative burst (study in *C. reinhardtii*) and disturb the gene expression during astaxanthin biosynthesis, it is still unable to leading the astaxanthin accumulation massively. Then we come to one question: what is the difference between nsPEFs stimulation and other abiotic stress to *H. pluvialis* on astaxanthin biosynthesis?

To study the abiotic stress on astaxanthin formation, we used salt stress to trigger the astaxanthin accumulation in 5 days old *H. pluvialis*. We observed that, 200 mM NaCl could induce an obvious astaxanthin accumulation than 100 mM NaCl (**Fig. 3.9B**), this is because 200 mM NaCl triggered the oxidative burst (**Fig. 3.9C**), which activated the secondary-defense strategy to against ROS formation (Li *et al.*, 2008). And maybe also because the ROS generated by salt stress, an increase of cell mortality in *H. pluvialis* was observed (**Fig. 3.9D**).

During the conversion from β-carotene into free astaxanthin, enzymes *crtR-b* and *bkt 1* will competes with each other to produce different middle by-products (**Fig. 1.7**). By comparing the gene expression of *crtR-b* and *bkt 1* between nsPEFs and salt treatment, we concluded a similar result, which enzyme BKT 1 was more necessary and competitive than *crtR-b* (**Fig. 3.8B,C** and **Fig. 3.10B,C**) during the biosynthesis of astaxanthin. Salt stress as a long-term stress condition existed in *H. pluvialis*, which could initiate the astaxanthin accumulation to against this persistent stress factor. While,

although nsPEFs could also disrupt the gene expression of *psy*, *crtR-b* and *bkt 1*, it is not effective to manipulate the balance between *crtR-b* and *bkt 1* into a benefit proportion, and finally leading to a massive biosynthesis of astaxanthin.

5. Conclusions

We have investigated the role of oxidative burst for the cellular responses induced by nsPEFs, both, short-term and long term nsPEFs. We found that nsPEFs could induce a rapid and transient increase of membrane permeability, followed by a transient volume increase, and slower lipid peroxidation. Furthermore, these responses were enhanced when the pulse duration increased from 25 ns to 50 ns. When the long-term response to nsPEFs were investigated, we observed an arrest of the cell cycle, a stimulation of cell expansion and a stimulated formation of palmella stages, correlated with a persistent long-term increasing of lipid peroxidation. While the spontaneous formation of palmella stages could be suppressed by exogenous IAA, the palmella formation in response to nsPEFs was not responsive to exogenous auxin. Our data show that nsPEFs release a long-lasting signal that persists, although the immediate cellular changes to the treatment are mostly reversed in the first two hours after pulsing. This persistent signal becomes manifest only days later and orchestrates a developmental reprogramming, which under natural conditions functions in the context of osmotic adaptation.

As nsPEFs could generate a long-lasting oxidative burst and force *C. reinhardtii* to turn into stress condition and form palmella stage, we performed nsPEFs on another microalgae *H. pluvialis* which could accumulate a highly antioxidative compound named astaxanthin when suffering oxidative burst or abiotic stress. We observed that nsPEFs could generate a long-term of cell mortality on *H. pluvialis*, and the extent sharply increased as the pulse duration/input energy increased from 25 ns/2 J·g^{-1} to 50 ns/4 J·g^{-1}. nsPEFs also triggered a long-term cell enlargement, but there was only a transient and slightly increase of astaxanthin accumulation at 48 h after 50 ns treatment. The gene expression of *psy*, *crtR-b* and *bkt 1* was transiently stimulated by nsPEFs on transcript level. And the peak expression of all three genes appeared within

48 h by 25 ns treatment and at 72 h by 50 ns. By using salt stress to trigger the astaxanthin accumulation in *H. pluvialis*, we concluded that 200 mM NaCl was able to stimulate the astaxanthin biosynthesis which may related to oxidative burst, but also accompanied with an intense of cell mortality. In comparison to the relative gene expression of *psy, crtR-b* and *bkt 1* during the astaxanthin biosynthesis between nsPEFs and salt stress treatment, the expression of gene *psy*, *crtR-b* and *bkt 1* could in response to both nsPEFs and salt stress treatment, however, gene *bkt 1* was more inducible than *psy* and *crtR-b* on transcript level, and this preferred induction of gene *bkt 1* maybe a key point in contribution to the massive astaxanthin biosynthesis in *H. pluvialis* when facing stress conditions.

6. Outlook

6.1. Further study in *C. reinhardtii*

In the study of long-term cell response of *C. reinhardtii* to nsPEFs, the still unknown signal that released by nsPEFs unfolds its effect only several days later, and therefore must be very stable. This signal obviously persists over several rounds of cell division, which means that it has to be regenerated during each cycle to remain stable. A mere alteration of the membrane induced by nsPEFs should be diluted by a factor of 2 during each cell cycle. A candidate for such a mechanism would be stable alterations of chromatin structure leading to changes in gene expression. Future work will therefore be directed to measure the response of gene expression to nsPEFs and to understand the epigenetic changes underlying such responses.

6.2. ROS signaling activated by nsPEFs in *H. pluvialis*

Although nsPEFs could generate a series of cell responses and trigger a persistent oxidative burst several days later in *C. reinhardtii*, it is fail for nsPEFs to become an abiotic stress like salt to induce a long-term astaxanthin biosynthesis and accumulation in *H. pluvialis*. In the study of *C. reinhardtii* in response to nsPEFs, we found that the NADPH-oxidase RboH was involved in the formation of oxidative burst induced by nsPEFs. Then we come to a question: whether the RboH could also be activated by nsPEFs in *H. pluvialis* and involved in the signal transduction in initiation of the astaxanthin biosynthesis? To testify this hypothesis, DPI could be added prior to the nsPEFs treatment to block the activity of RboH, and the astaxanthin accumulation and gene expression are quantified to determine the role of RboH played in *H. pluvialis*. And a preliminary result was shown in **Fig. 6.1**.

According to the preliminary result in **Fig. 6.1**, we found out that, after inhibited the activity of NADPH-oxidase RboH, the astaxanthin content and gene expression were all induced in control and pulse treatment. And it seems that RboH play a negative role in astaxanthin biosynthesis. So our further work will focus on the role of RboH and other signaling molecules such as calcium in the astaxanthin biosynthesis after nsPEFs treatment.
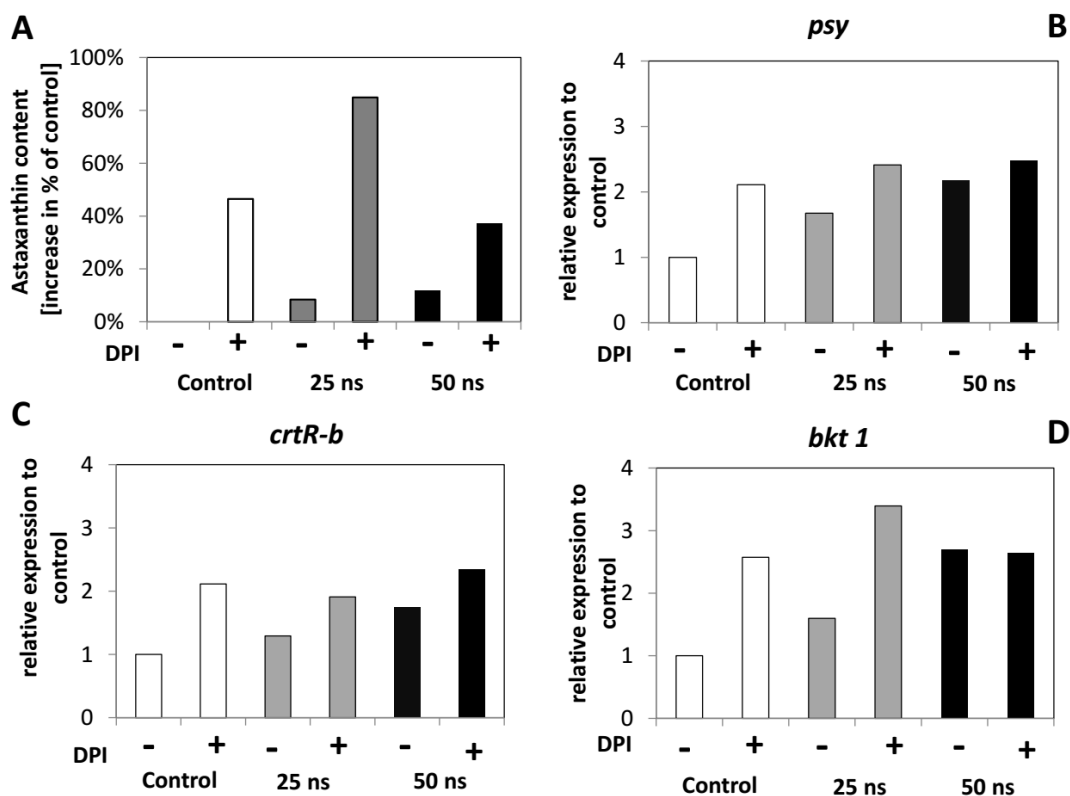
Figure 6.1: Role of NADPH-oxidase RboH for the astaxanthin gene expression and biosynthesis in response to nsPEFs treatment. **A** Astaxanthin content presented by the increase % of control. **B** Relative expression of *psy* to control. **C** Relative expression of *crtR-b* to control. **D** Relative expression of *bkt 1* to control. DPI (8 µM as final concentration in experiment) was added 30 min prior to administering the nsPEFs treatment in 5 days old *H. pluvialis*. And the astaxanthin content and gene expression were quantified at 72 h after pulse treatment.

References

Akiyama, H.&Heller, R. (2016). Bioelectrics. *Springer Japan*

Anderberg, H.I., Danielson, J.Å.&Johanson, U. (2011). Algal MIPs, high diversity and conserved motifs. *BMC Evol. Biol.* **11**, 110.

Andrewes, A.G., Phaff, H.J.&Starr, M.P. (1976). Carotenoids of *Phaffia rhodozyma*, a red-pigmented fermenting yeast. *Phytochemistry* **15**, 1003-1007.

Beebe, S.J., Chen, Y.J., Sain, N.M., Schoenbach, K.H.&Xiao, S. (2012). Transient features in nanosecond pulsed electric fields differentially modulate mitochondria and viability. *PLoS ONE* **7**, e51349.

Bennedsen, M., Wang, X., Willén, R., Wadström, T.&Andersen, L.P. (2000). Treatment of *H. pylori* infected mice with antioxidant astaxanthin reduces gastric inflammation, bacterial load and modulates cytokine release by splenocytes. *Immunology Lett.* **70**, 185-189.

Berghöfer, T., Eing, C., Flickinger, B., Hohenberger, P., Wegner, L.H., Frey, W.&Nick, P. (2009). Nanosecond electric pulses trigger actin responses in plant cells. *Biochem. Biophys. Res. Commun.* **387**, 590-595.

Bhattacharjee, S. (2005). Reactive oxygen species and oxidative burst: roles in stress, senescence and signal transduction in plants. *Curr. Sci.* **89**, 1113-1121.

Boussiba, S. (2000). Carotenogenesis in the green alga *Haematococcus pluvialis*: cellular physiology and stress response. *Physiol. Plant.* **108**, 111-117.

Boussiba, S., Bing, W., Yuan, J.P., Zarka, A.&Chen, F. (1999). Changes in pigments profile in the green alga *Haeamtococcus pluvialis* exposed to environmental stresses. *Biotechnol. Lett.* **21**, 601-604.

Boussiba, S.&Vonshak, A. (1991). Astaxanthin accumulation in the green alga *Haematococcus pluvialis*. *Plant Cell Physiol.* **32**, 1077-1082.

Breton, M., Delemotte, L., Silve, A., Mir, L.M.&Tarek, M. (2012). Transport of siRNA through lipid membranes driven by nanosecond electric pulses: an experimental and computational study. *J. Am. Chem. Soc.* **134**, 13938-13941.

Campanoni, P. (2005). Auxin-dependent cell division and cell elongation.

References

1-naphthaleneacetic acid and 2,4-dichlorophenoxyacetic acid activate different pathways. *Plant Physiol.* **137**, 939-948.

Chang, X.L., Riemann, M., Liu, Q.&Nick, P. (2015). Actin as deathly switch? How auxin can suppress cell-death related defence. *PLoS ONE* **10**, journal.pone.0125498.

Chen, C., Smye, S.W., Robinson, M.P.&Evans, J.A. (2006). Membrane electroporation theories: a review. *Med. Biol. Eng. Comput.* **44**, 5-14.

Chen, G., Wang, B., Han, D., Sommerfeld, M., Lu, Y., Chen, F.&Hu, Q. (2015). Molecular mechanisms of the coordination between astaxanthin and fatty acid biosynthesis in *Haematococcus pluvialis* (Chlorophyceae). *Plant J.* **81**, 95-107.

Chen, N.Y., Schoenbach, K.H., Kolb, J.F., Swanson, R.J., Garner, A.L., Yang, J., Joshi, R.P.&Beebe, S.J. (2004). Leukemic cell intracellular responses to nanosecond electric fields. *Biochem. Biophys. Res. Commun.* **317**, 421-427.

Chen, X.H., Beebe, S.J.&Zheng, S.S. (2012). Tumor ablation with nanosecond pulsed electric fields. *HBPD Int.* **11**, 122-124.

Christiansen, R., Lie, O.&Torrissen, O.J. (1995). Growth and survival of Atlantic salmon, *Salmo salar* L., fed different dietary levels of astaxanthin. First-feeding fry. *Aquac. Nutr.* **1**, 189-198.

Cross, A.R.&Jones, O.T.G. (1986). The effect of the inhibitor diphenylene iodonium on the superoxide-generating   system of neutrophils. *Biochem. J.* **237**, 111-116.

De Smet, I., Voß, U., Lau, S., Wilson, M., Shao, N., Timme, R.E., Swarup, R., Kerr, I., Hodgman, C., Bock, R., Bennett, M., Jürgens, G.&Beeckman, T. (2011). Unraveling the evolution of auxin signaling. *Plant Physiol.* **155**, 209-221.

Dubiella, U., Seybold, H., Durian, G., Komander, E., Lassig, R., Witte, C.P., Schulze, W.X.&Romeis, T. (2013). Calcium-dependent protein kinase/NADPH oxidase activation circuit is required for rapid defense signal propagation. *PNAS* **110**, 8744-8749.

Eing, C.J., Bonnet, S., Pacher, M., Puchta, H.&Frey, W. (2009). Effects of nanosecond pulsed electric field exposure on *Arabidopsis thaliana*. *IEEE Trans. Dielectr. Electr. Insul.* **16**, 1322-1328.

Erickson, E., Wakao, S.&Niyogi, K.K. (2015). Light stress and photoprotection in

Chlamydomonas reinhardtii. Plant J. **82**, 449-465.

Escoffre, J.M., Bellard, E., Faurie, C., Sebai, S.C., Golzio, M., Teissie, J.&Rols, M.P. (2014). Membrane disorder and phospholipid scrambling in electropermeabilized and viable cells. *BBA - Biomembranes* **1838**, 1701-1709.

Fassett, R.G.&Coombes, J.S. (2012). Astaxanthin in cardiovascular health and disease. *Molecules* **17**, 2030-2048.

Fehér, A., Ötvös, A., Pasternak, T.P.&Szandtner, A.P. (2008). The involvement of reactive oxygen species (ROS) in the cell cycle activation (G0-to-G1 transition) of plant cells. *Plant Signal. Behav.* **3**, 823-826.

Flickinger, B., Berghöfer, T., Hohenberger, P., Eing, C.&Frey, W. (2010). Transmembrane potential measurements on plant cells using the voltage-sensitive dye ANNINE-6. *Protoplasma* **247**, 3-12.

Forman, H.J.&Boveris, A. (1982). Superoxide radical and hydrogen peroxide in mitochondria. *Free Radic. Biol. Med.* **5**, 65-90.

Frank, H.A.&Cogdell, R.J. (1996). Carotenoids in photosynthesis. *Photochem. Photobiol.* **63**, 257-264.

Gaff, D.F.&Okong'O-Ogola, O. (1971). The use of non-permeating pigments for testing the survival of cells. *J. Exp. Bot.* **22**, 756-758.

Goettel, M., Eing, C., Gusbeth, C., Straessner, R.&Frey, W. (2013). Pulsed electric field assisted extraction of intracellular valuables from microalgae. *Algal Res.* **2**, 401-408.

Gorman, D.S.&Levine, R.P. (1965). Cytochrome f and plastocyanin: their sequence in thephotosynthetic electron transport chain of *Chlamydomonas reinhardi*. *Proc. Natl. Acad. Sci.* **54**, 1665-1669.

Gowrishankar, T.R., Esser, A.T., Vasilkoski, Z., Smith, K.C.&Weaver, J.C. (2006). Microdosimetry for conventional and supra-electroporation in cells with organelles. *Biochem. Biophys. Res. Commun.* **341**, 1266-1276.

Grunewald, K., Hirschberg, J.&Hagen, C. (2001). Ketocarotenoid biosynthesis outside of plastids in the unicellular green alga *Haematococcus pluvialis*. *J. Biol. Chem.* **276**, 6023-6029.

References

Guerin, M., Huntley, M.E.&Olaizola, M. (2003). *Haematococcus* astaxanthin: applications for human health and nutrition. *Trends Biotechnol.* **21**, 210-216.

Guionet, A., Hosseini, B., Teissie, J., Akiyama, H.&Hosseini, H. (2017). A new mechanism for efficient hydrocarbon electro-extraction from *Botryococcus braunii*. *Biotechnol Biofuels.* **10**, 39.

Harris, E.H. (1989). The *Chlamydomonas* sourcebook: a comprehensive guide to biology and laboratory use. *Academic Press, San Diego California*

He, L., Xiao, D., Feng, J., Yao, C.&Tang, L. (2017). Induction of apoptosis of liver cancer cells by nanosecond pulsed electric fields (nsPEFs). *Med. Oncol.* **34**, 24.

Henderson, L.M.&Chappell, J.B. (1993). Dihydrorhodamine 123: a fluorescent probe for superoxide generation? *Eur. J. Biochem.* **217**, 973-980.

Hodgson, R.A.J.&Raison, J.K. (1991). Lipid peroxidation and superoxide dismutase activity in relation to photoinhibition induced by chilling in moderate light. *Planta* **185**, 215-219

Hohenberger, P., Eing, C., Straessner, R., Durst, S., Frey, W.&Nick, P. (2011). Plant actin controls membrane permeability. *BBA - Biomembranes* **1808**, 2304-2312.

Holtin, K., Kuehnle, M., Rehbein, J., Schuler, P., Nicholson, G.&Albert, K. (2009). Determination of astaxanthin and astaxanthin esters in the microalgae *Haematococcus pluvialis* by LC-(APCI)MS and characterization of predominant carotenoid isomers by NMR spectroscopy. *Anal. Bioanal. Chem.* **395**, 1613-1622.

Huang, J.C., Chen, F.&Sandmann, G. (2006). Stress-related differential expression of multiple beta-carotene ketolase genes in the unicellular green alga *Haematococcus pluvialis. J. Biotechnol.* **122**, 176-185.

Huang, J.C., Zhong, Y.J., Liu, J., Sandmann, G.&Chen, F. (2013). Metabolic engineering of tomato for high-yield production of astaxanthin. *Metab. Eng.* **17**, 59-67.

Jürgen, B.H. (2013). Do we age because we have mitochondria? *Protoplasma* **251**, 3-23.

Janero, D.R. (1990). Malondialdehyde and thiobarbituric acid-reactivity as diagnostic indices of lipid peroxidation and peroxidative tissue injury. *Free Radic. Biol. Med.* **9**, 515-540.

Kühn, S., Liu, Q., Eing, C., Frey, W.&Nick, P. (2013). Nanosecond electric pulses affect a plant-specific kinesin at the plasma membrane. *J. Membr. Biol.* **246**, 927-938.

Kajiwara, S., Kakizono, T., Saito, T., Kondo, K., Ohtani, T., Nishio, N., Nagai, S.&Misawa, N. (1995). Isolation and functional identification of a novel cDNA for astaxanthin biosynthesis from *Haematococcus pluvialis*, and astaxanthin synthesis in *Escherichia coli. Plant Mol. Biol.* **29**, 343-352.

Kakizono, T., Kobayashi, M.&Nagal, S. (1992). Effect of carbon/nitrogen ratio on encystment accompanied with astaxanthin formation in a green alga. *J. Ferment. Bioeng.* **74**, 403-405.

Kinosita, K.&Tsong, T.Y. (1977). Formation and resealing of pores of controlled sizes in human erythrocyte membrane. *Nature* **268**, 438-441.

Kobayashi, M., Kakizono, T.&Nagal, S. (1991). Astaxanthin production by a green alga, *Haematococcus pluvialis* accompanied with morphological changes in acetate media. *J. Ferment. Bioeng.* **71**, 335-339.

Kobayashi, M., Kakizono, T., Nishio, N., Nagai, S., Kurimura, Y.&Tsuji, Y. (1997a). Antioxidant role of astaxanthin in the green alga *Haematococcus pluvialis. Appl. Microbiol. Biotechnol.* **48**, 351-356.

Kobayashi, M., Kurimura, Y.&Tsuji, Y. (1997b). Light-independent, astaxanthin production by the green microalga *Haematococcus pluvialis* under salt stress. *Biotechnol. Lett.* **19**, 507-509.

Kudla, J., Batistič, O.&Hashimoto, K. (2010). Calcium signals: the lead currency of plant information processing. *Plant Cell* **22**, 541-563.

Lakshmanan, S., Gupta, G.K., Avci, P., Chandran, R., Sadasivam, M., Jorge, A.E.&Hamblin, M.R. (2014). Physical energy for drug delivery; poration, concentration and activation. *Adv. Drug Deliv. Rev.* **71**, 98-114.

Lemoine, Y.&Schoefs, B. (2010). Secondary ketocarotenoid astaxanthin biosynthesis in algae: a multifunctional response to stress. *Photosyn. Res.* **106**, 155-177.

Li, Y., Sommerfeld, M., Chen, F.&Hu, Q. (2008). Consumption of oxygen by astaxanthin biosynthesis: a protective mechanism against oxidative stress in *Haematococcus pluvialis*

References

(Chlorophyceae). *J. Plant Physiol.* **165**, 1783-1797.

Linden, H. (1999). Carotenoid hydroxylase from *Haematococcus pluvialis*: cDNA sequence, regulation and functional complementation. *BBA-Gene Struct. Expr.* **1446**, 203-212.

Lorenz, R.T.&Cysewski, G.R. (2000). Commercial potential for *Haematococcus* microalgae as a natural source of astaxanthin. *Trends Biotechnol.* **18**, 160-167.

Loschen, G., Azzi, A.&Flohé, L. (1973). Mitochondrial H_2O_2 formation: relationship with energy conservation. *FEBS Lett.* **33**, 84-88.

Lotan, T.&Hirschberg, J. (1995). Cloning and expression in *Escherichia coli* of the gene encoding β-C-4-oxygenase, that converts β-carotene to the ketocarotenoid canthaxanthin in *Haematococcus pluvialis*. *FEBS Lett.* **364**, 125-128.

Lu, Y., Jiang, P., Liu, S., Gan, Q., Cui, H.&Qin, S. (2010). Methyl jasmonate- or gibberellins A3-induced astaxanthin accumulation is associated with up-regulation of transcription of beta-carotene ketolase genes (bkts) in microalga *Haematococcus pluvialis*. *Bioresour. Technol.* **101**, 6468-6474.

Marino, D., Dunand, C., Puppo, A.&Pauly, N. (2012). A burst of plant NADPH oxidases. *Trends Plant Sci.* **17**, 9-15.

Mehdy, M.C. (1994). Active oxygen species in plant defense against pathogens. *Plant Physiol.* **105**, 467-472

Miao, X., Yin, S., Shao, Z., Zhang, Y.&Chen, X. (2015). Nanosecond pulsed electric field inhibits proliferation and induces apoptosis in human osteosarcoma. *J. Orthop. Surg. Res.* **10**, 104.

Miller, G., Suzuki, N., Sultan, C.Y.&Mittler, R. (2010). Reactive oxygen species homeostasis and signalling during drought and salinity stresses. *Plant Cell Environ.* **33**, 453-467.

Mir, L.M., Orlowski, S., Jean, B.J.&Paoletti, C. (1991). Electrochemotherapy potentiation of antitumour effect of bleomycin by local electric pulses. *Europ. J. Cancer. Clin. Oncol.* **27**, 68-72.

Morotomi-Yano, K., Akiyama, H.&Yano, K. (2011a). Nanosecond pulsed electric fields

activate MAPK pathways in human cells. *Arch. Biochem. Biophys.* **515**, 99-106.

Morotomi-Yano, K., Akiyama, H.&Yano, K. (2012). Nanosecond pulsed electric fields activate AMP-activated protein kinase: implications for calcium-mediated activation of cellular signaling. *Biochem. Biophys. Res. Commun.* **428**, 371-375.

Morotomi-Yano, K., Uemura, Y., Katsuki, S., Akiyama, H.&Yano, K. (2011b). Activation of the JNK pathway by nanosecond pulsed electric fields. *Biochem. Biophys. Res. Commun.* **408**, 471-476.

Nappi, A.J.&Vass, E. (2000). Hydroxyl radical production by ascorbate and hydrogen peroxide. *Neurotox. Res.* **2**, 343-355.

Nesin, O.M., Pakhomova, O.N., Xiao, S.&Pakhomov, A.G. (2011). Manipulation of cell volume and membrane pore comparison following single cell permeabilization with 60- and 600-ns electric pulses. *BBA - Biomembranes* **1808**, 792-801.

Neumann, E.&Rosenheck, K. (1972). Permeability changes induced by electric impulses in vesicular membranes. *J. Membr. Biol.* **10**, 279-290.

Noctor, G.&Foyer, C.H. (1998). Ascorbate and glutathione: keeping active oxygen under control. *Annu. Rev. Plant Physiol. Plant Mol. Biol.* **49**, 249-279.

Orosa, M., Torres, E., Fidalgo, P.&Abalde, J. (2000). Production and analysis of secondary carotenoids in green algae. *J. Appl. Phycol.* **12**, 553-556.

Pakhomov, A.G., Xiao, S., Pakhomova, O.N., Semenov, I., Kuipers, M.A.&Ibey, B.L. (2014). Disassembly of actin structures by nanosecond pulsed electric field is a downstream effect of cell swelling. *Bioelectrochemistry* **100**, 88-95.

Pakhomova, O.N., Khorokhorina, V.A., Bowman, A.M., Rodaitė-Riševičienė, R., Saulis, G., Xiao, S.&Pakhomov, A.G. (2012). Oxidative effects of nanosecond pulsed electric field exposure in cells and cell-free media. *Arch. Biochem. Biophys.* **527**, 55-64.

Proschold, T. (2005). Portrait of a Species: *Chlamydomonas reinhardtii. Genetics* **170**, 1601-1610.

Raja, R., Hemaiswarya, S.&Rengasamy, R. (2007). Exploitation of *Dunaliella* for β-carotene production. *Appl. Microbiol. Biotechnol.* **74**, 517-523.

Ralley, L., Enfissi, E.M., Misawa, N., Schuch, W., Bramley, P.M.&Fraser, P.D. (2004).

Metabolic engineering of ketocarotenoid formation in higher plants. *Plant J.* **39**, 477-486.

Remias, D., Lütz-Meindl, U.&Lütz, C. (2005). Photosynthesis, pigments and ultrastructure of the alpine snow alga *Chlamydomonas nivalis*. *Eur. J. Phycol.* **40**, 259-268.

Rochaix, J.D. (1995). *Chlamydomonas reinhardtii* as the photosynthetic yeast. *Annu. Rev. Genet.* **29**, 209-230.

Rochaix, J.D. (2002). *Chlamydomonas*, a model system for studying the assembly and dynamics of photosynthetic complexes. *FEBS Lett.* **529**, 34-38.

Sabri, N., Pelissier, B.&Teissie, J. (1996). Electropermeabilization of intact maize cells induces an oxidative stress. *Eur. J. Biochem.* **238**, 737-743.

Sack, M., Sigler, J., Frenzel, S., Eing, C., Arnold, J., Michelberger, T., Frey, W., Attmann, F., Stukenbrock, L.&Müller, G. (2010). Research on industrial-scale electroporation devices fostering the extraction of substances from biological tissue. *Food Eng. Rev.* **2**, 147-156.

Sagi, M. (2006). Production of reactive oxygen species by plant NADPH oxidases. *Plant Physiol.* **141**, 336-340.

Sahoo, D.&Seckbach, J. (2015). The algae world. *Springer, Berlin Heidelberg New York*

Sauer, H., Wartenberg, M.&Hescheler, J. (2001). Reactive oxygen species as intracellular messengers during cell growth and differentiation. *Cell Physiol. Biochem.* **11**, 173-186.

Scarlett, S.S., White, J.A., Blackmore, P.F., Schoenbach, K.H.&Kolb, J.F. (2009). Regulation of intracellular calcium concentration by nanosecond pulsed electric fields. *BBA - Biomembranes* **1788**, 1168-1175.

Schoenbach, K.H., Joshi, R.P., Kolb, J.F., Chen, N.Y., Stacey, M., Blackmore, P.F., Buescher, E.S.&Beebe, S.J. (2004). Ultrashort electrical pulses open a new gateway into biological cells. *Proc. IEE* **92**, 1122-1137.

Shimidzu, N., Goto, M.&Miki, W. (1996). Carotenoids as singlet oxygen quenchers in marine organisms. *Fisheries Sci.* **62**, 134-137.

Silflow, C.D.&Lefebvre, P.A. (2001). Assembly and motility of eukaryotic cilia and flagella.

Lessons from *Chlamydomonas reinhardtii*. *Plant Physiol.* **127**, 1500-1507.

Skjånes, K., Rebours, C.&Lindblad, P. (2012). Potential for green microalgae to produce hydrogen, pharmaceuticals and other high value products in a combined process. *Crit. Rev. Biotechnol.* **33**, 172-215.

Spolaore, P., Joannis Cassan, C., Duran, E.&Isambert, A. (2006). Commercial applications of microalgae. *J. Biosci. Bioeng.* **101**, 87-96.

Steinbrenner, J.&Linden, H. (2001). Regulation of two carotenoid biosynthesis genes coding for phytoene synthase and carotenoid hydroxylase during atress-induced astaxanthin formation in the green alga *Haematococcus pluvialis*. *Plant Physiol.* **125**, 810-817.

Steinbrenner, J.&Sandmann, G. (2006). Transformation of the green alga *Haematococcus pluvialis* with a phytoene desaturase for accelerated astaxanthin biosynthesis. *Appl. Environ. Microbiol.* **72**, 7477-7484.

Takaki, K., Yamazaki, N., Mukaigawa, S., Fujiwara, T., Kofujita, H., Takahasi, K., Narimatsu, M.&Nagane, K. (2009). Improvement of edible mushroom yield by electric stimulations. *JPFR-S* **8**, 556-559.

Tanaka, T., Morishita, Y., Suzui, M., Kojima, T., Okumura, A.&Mori, H. (1994). Chemoprevention of mouse urinary bladder carcinogenesis by the naturally occurring carotenoid astaxanthin. *Carcinogenesis* **15**, 15-19.

Triantaphylidès, C.&Havaux, M. (2009). Singlet oxygen in plants: production, detoxification and signaling. *Trends Plant Sci.* **14**, 219-228.

Tsubokura, A., Yoneda, H.&Mizuta, H. (1999). *Paracoccus carotinifaciens* sp. nov., a new aerobic Gram-negative astaxanthin-producing bacterium. *Int. J. Syst. Evol. Microbiol.* **49**, 277-282.

Varghese, B.&Naithani, S.C. (2008). Oxidative metabolism-related changes in cryogenically stored neem (*Azadirachta indica* A. Juss) seeds. *J. Plant Physiol.* **165**, 755-765.

Wan, M.X., Zhang, J.K., Hou, D.M., Fan, J.H., Li, Y.G., Huang, J.K.&Wang, J. (2014). The effect of temperature on cell growth and astaxanthin accumulation of *Haematococcus*

pluvialis during a light–dark cyclic cultivation. *Bioresour. Technol.* **167**, 276-283.

Wegner, L.H., Flickinger, B., Eing, C., Berghöfer, T., Hohenberger, P., Frey, W.&Nick, P. (2011). A patch clamp study on the electro-permeabilization of higher plant cells: supra-physiological voltages induce a high-conductance, K^+ selective state of the plasma membrane. *BBA - Biomembranes* **1808**, 1728-1736.

Wojtaszek, P. (1997). Oxidative burst: an early plant response to pathogen infection. *Biochem. J.* **322**, 681-692.

Wolfe, J., Dowgert, M.F.&Steponkus, P.L. (1986). Mechanical study of the deformation and rupture of the plasma membranes of protoplasts during osmotic expansions. *J. Membr. Biol.* **93**, 63-74.

Wouters, P.C.&Smelt, J.P.P.M. (1997). Inactivation of microorganisms with pulsed electric fields: potential for food preservation. *Food Biotechnol.* **11**, 193-229.

Wu, H.M., Hazak, O., Cheung, A.Y.&Yalovsky, S. (2011). RAC/ROP GTPases and auxin signaling. *Plant Cell* **23**, 1208-1218.

Xia, X.J., Zhou, Y.H., Shi, K., Zhou, J., Foyer, C.H.&Yu, J.Q. (2015). Interplay between reactive oxygen species and hormones in the control of plant development and stress tolerance. *J. Exp. Bot.* **66**, 2839-2856.

Yano, M., Abe, K., Katsuki, S.&Akiyama, H. (2011) Gene expression analysis of apoptosis pathway in HeLa S3 cells subjected to nanosecond pulsed electric fields. *In* 2011 IEEE Pulsed Power Conference, pp 1221-1225

Yokoyama, A.&Miki, W. (1995). Composition and presumed biosynthetic pathway of carotenoids in the astaxanthin-producing bacterium *Agrobacterium aurantiacum*. *FEMS Microbiol. Lett.* **128**, 139-144.

Zhang, D.H., Ng, Y.K.&Phang, S.M. (1997). Composition and accumulation of secondary carotenoids in *Chlorococcum sp. J. Appl. Phycol.* **9**, 147-155.

7. Appendix

7.1. Different light sources influence the cell growth and astaxanthin accumulation in *H. pluvialis*

To investigate the growth distribution and the accumulation of astaxanthin in *H. pluvialis* under irradiation stress. Cell suspensions were cultivated under white (control), red and blue light separately for 14 days. The control group was cultivated under white illumination light (L 36W/965; OSRAM, Germany), the red and blue light sources were self-made LED array, and the details were shown in **Table 7.1**. The cell suspensions were inoculated into 30 ml basal medium and cultivated in the incubators with corresponding light sources, the cultivation temperature was 25 ℃ and the algae was manually shaking once per day. To get insight into the growth distribution of *H. pluvialis* in response to different light irradiations, the cell density (OD_{750}), cell mortality, cell diameter and astaxanthin content were quantified every day (**Fig. 7.1**).

Table 7.1 Basic parameters of light sources

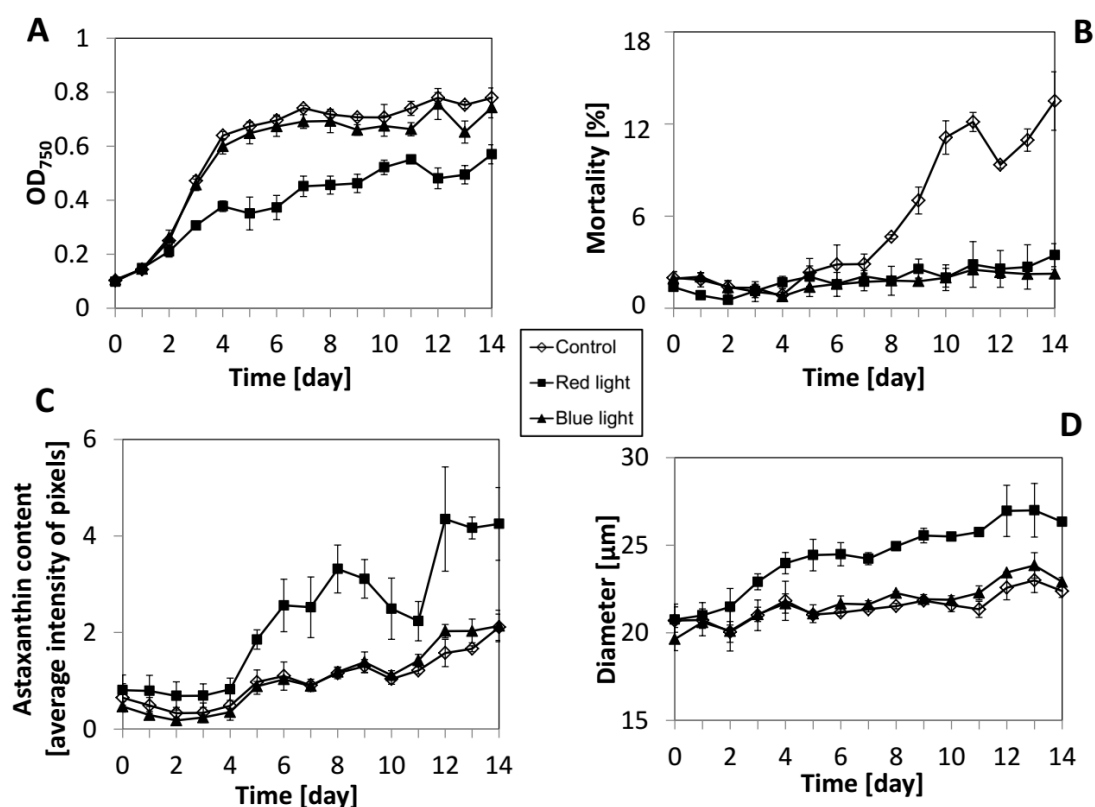|	Wavelength (nm)	Max wavelength (nm)	Light intensity ($\mu mol \cdot m^{-2} \cdot s^{-1}$)	Energy ($W \cdot m^{-2}$)
White (Control)	400-700	550	57	12
Red light	600-700	650	65	12
Blue light	430-530	470	47	12

Figure 7.1: The *H. pluvialis* growth distribution and astaxanthin accumulation in response to white, red and blue light sources. **A** Cell density was measured as the read out of OD_{750}. **B** Cell mortality was measured as the percentage of dead cells stained by membrane impermeable dye Evan's Blue. **C** Astaxanthin content was represented by the average intensity of pixels of astaxanthin signal quantified by Image J software. **D** Cell diameter was measured as the read out of cell expansion. Data represent mean values, error bars s_e of three independent experimental replications.

The results of *H. pluvialis* in response to different light irradiations showed that, red light source could obvious inhibit the growth of *H. pluvialis* compared to control and blue light (**Fig. 7.1A**), however, red light was benefit for the astaxanthin accumulation and increased the cell viability than white and blue light (**Figs. 7.B,C**). For the cells cultivated under blue light, the cell mortality was inhibited after 7 days cultivation in comparison to control (**Fig. 7.1B**), but there was not stimulation on the growth and astaxanthin accumulation (**Figs.**

7.1A,C,D).

7.2. Long-term salt stress influence the cell growth and astaxanthin accumulation in *H. pluvialis*

To found out the growth distribution and the astaxanthin accumulation of *H. pluvialis* in response to a long-term salt stresses. 30 ml basal medium with NaCl in final concentration of 0 (control), 50, 100, 150 and 200 mM were used to cultivate cells for 14 days. The cultivation temperature was 25 ℃ with continuous white illumination light (L 36W/965; OSRAM, Germany) of 25 $\mu mol \cdot m^{-2} \cdot s^{-1}$ light intensity, and the cells were manually shaking once per day. To verify the growth distribution of *H. pluvialis* in response to different concentration of salt stress, the cell density (OD_{750}), cell mortality, cell diameter and astaxanthin content were determined every day (**Fig. 7.2**).

We found out that, in comparison to control, the cell density was seriously inhibited as the NaCl concentration increased (**Fig. 7.2A**). However, as the salt stress enhancement, the astaxanthin content and cell expansion in *H. pluvialis* were increased (**Figs. 7.2C,D**). But the higher NaCl concentration also causing a serious stress condition and leading to an increase of cell mortality (**Fig. 7.2B**).
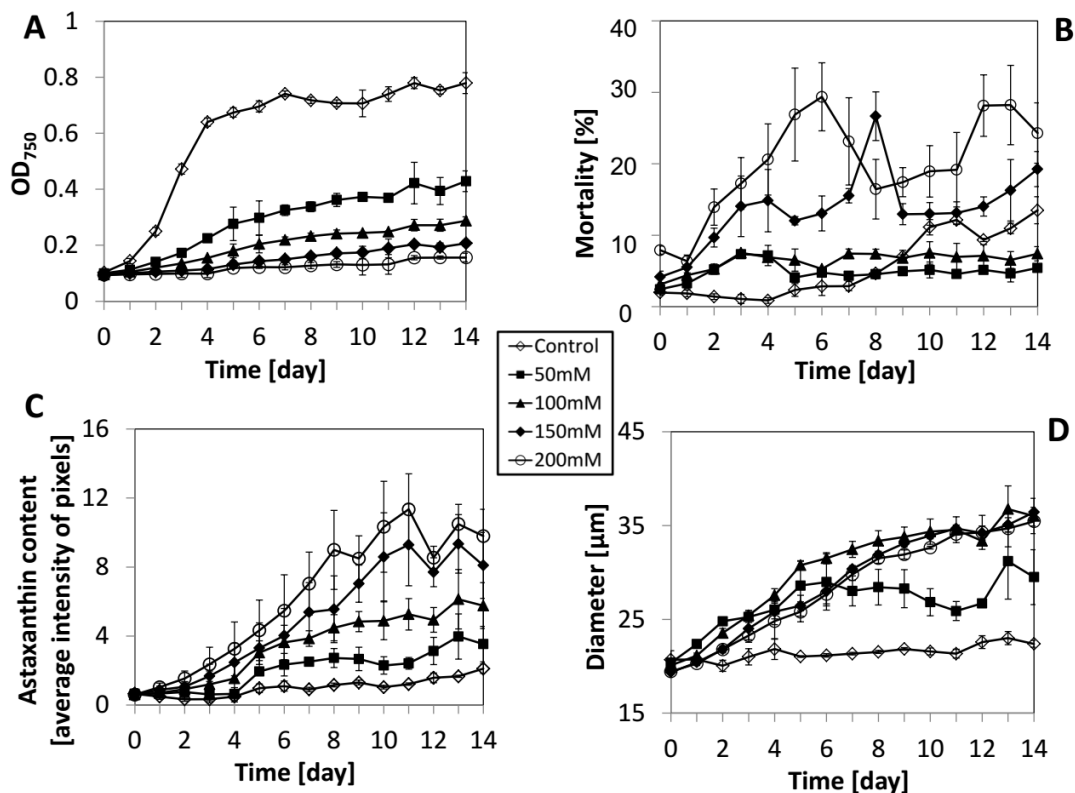
Figure 7.2: The *H. pluvialis* growth distribution and astaxanthin accumulation in response to different NaCl concentrations. **A** Cell density was measured as the read out of OD_{750}. **B** Cell mortality was measured as the percentage of dead cells stained by membrane impermeable dye Evan's Blue. **C** Astaxanthin content was represented by the average intensity of pixels of astaxanthin signal quantified by Image J software. **D** Cell diameter was measured as the read out of cell expansion. Data represent mean values, error bars s_e of three independent experimental replications.

Curriculum Vitae

PERSONAL DATA

Name: Fan Bai

Gender: Female

Nationality: P.R. China

Place of Birth: Jilin city, Jilin Province, P. R. China

Email: fan.bai@partner.kit.edu; baifan1215@aliyun.com

EDUCATION

10/2013- 07/2017 **Ph.D.** major in Molecular Cell Biology

Karlsruhe Institute of Technology (KIT), Botanical Institute, Germany

09/2010- 07/2013 **M.S.** major in Environmental Engineering

University of Chinese Academy of Sciences (UCAS), China

09/2006- 06/2010 **B.S.** major in Environmental Science

Jilin Agricultural University, China

PUBLICATIONS

Fan Bai, Christian Gusbeth, Wolfgang Frey, Peter Nick. **2017**. Nanosecond pulsed electric fields trigger cell differentiation in *Chlamydomonas reinhardtii*. *BBA-Biomembranes*, 1859: 651-661.